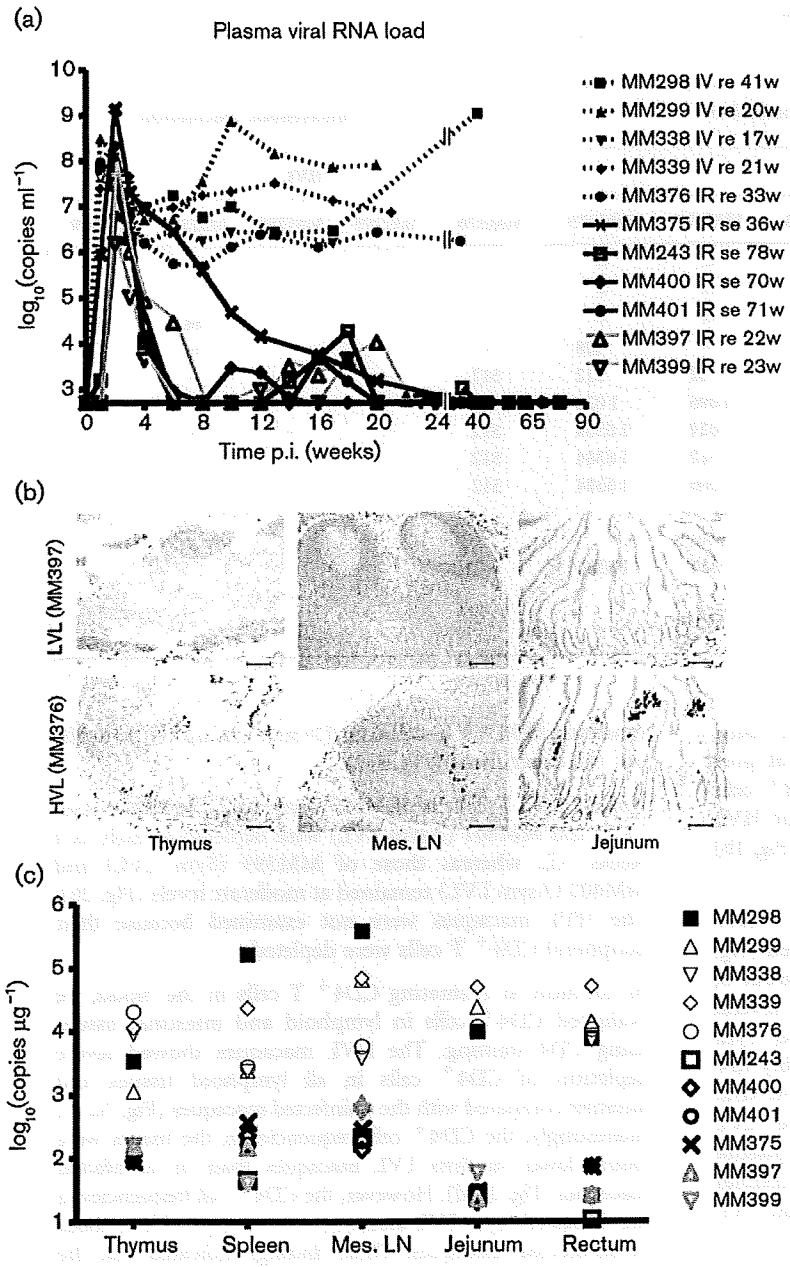

COLOUR FIGURE

Fig. 1. Distribution of virus in various tissues of SHIV-KS661-infected rhesus macaques. (a) Time course of plasma viral RNA loads as measured by quantitative RT-PCR. The detection limit of plasma viral RNA loads was 500 copies ml^{-1}. The animal ID numbers, infection route and when and how they were euthanized are indicated on the figure. IV, Intravenous inoculation; IR, intrarectal inoculation; re, required euthanasia; se, scheduled euthanasia; w, number of weeks after infection when euthanasia was performed. (b) Immunohistochemical detection of Nef antigen in thymus, mesenteric lymph nodes (Mes. LN) and jejunum. Brown staining indicates Nef^+ cells. The upper panels show representative tissue sections from a Sym LVL macaque (MM397) and the lower panels show representative tissue sections from an HVL macaque (MM376). Bars, 100 µm. (c) Proviral DNA loads in different tissues of SHIV-KS661-infected macaques, as measured by quantitative PCR. The detection limit of proviral DNA loads was 10 copies μg^{-1}. Filled black symbols indicate HVL macaques, open black symbols indicate Asym LVL macaques and open grey symbols indicate Sym LVL macaques.

macaques with diarrhoea and wasting symptomatic LVL macaques (Sym LVL).

Antibody response against SHIV in infected macaques

The LVL macaques showed antibody responses to SHIV-KS661 at 3–4 weeks p.i. and then developed strong antibody responses that persisted up to 18 weeks p.i. (Table 1). In contrast, two of the HVL macaques (MM298 and MM299) showed no antibody response, whilst the remaining two (MM338 and MM339) showed very low antibody responses. Among the HVL macaques, only MM376 showed a strong antibody response: the titre reached 1:2048 at 6 weeks p.i., but then decreased to a much lower value. These results showed that LVL macaques succeeded in maintaining a strong antibody response, whilst HVL macaques failed to do so.

Viral levels in tissues from Sym LVL and Asym LVL macaques are not significantly different

To investigate whether the infected macaques had different viral levels in their lymphoid and intestinal tissues, we used

Table 1. Anti-HIV antibody titres in infected monkeys

– indicates a titre of <32.

Time (weeks)	Intrarectal inoculation						Intravenous inoculation				
	LVL						HVL				
	MM243	MM397	MM399	MM400	MM401	MM375	MM376	MM298	MM299	MM338	MM339
0	–	–	–	–	–	–	–	–	–	–	–
1	–	–	–	–	–	–	–	–	–	–	–
2	–	–	–	–	–	–	–	–	–	64	64
3	32	–	32	–	–	128	–	–	–	32	32
4	32	16384	32	64	32	512	512	–	–	–	–
6	8192	16384	256	64	4096	1024	2048	–	–	–	–
8	4096	16384	1024	128	1024	16384	512	–	–	–	–
10	16384	16384	2048	512	512	16384	512	–	–	–	–
12	16384	16384	256	512	4096	16384	512				
13								–	–	–	–
14	16384	16384	1024	512	2048						
16	4096	8192	1024	1024	1024	16384	64				
17								–	–	–	–
18	8192	16384	2048	8192	4096						

the Nef antigen as a marker of virus infection using immunohistochemistry and quantitative analysis of proviral DNA in lymphoid and intestinal tissues. Nef$^+$ cells were detected in large numbers in the tissues of HVL macaques, but were undetectable in both Sym LVL (Fig. 1b) and Asym LVL (data not shown) macaques.

In the HVL macaques, high proviral DNA loads (>1000 copies μg^{-1}) were found in all of the tissues examined (Fig. 1c). In contrast, the proviral DNA loads in the tissues of the LVL macaques were only several tens to several hundreds of copies μg^{-1} (Fig. 1c). Furthermore, Sym LVL and Asym LVL macaques exhibited comparably low proviral DNA loads in these tissues (Fig. 1c). The low viral levels in lymphoid and intestinal tissues in the LVL macaques were consistent with their set points of plasma viral RNA loads. The viral levels in lymphoid and intestinal tissues were not significantly different between Sym LVL and Asym LVL macaques.

Diarrhoea and wasting in LVL macaques correlate with CD4$^+$ cell frequency in lymphoid and intestinal tissues, but not in peripheral blood

Because CD4$^+$ T-cell depletion is the hallmark of AIDS, we first examined CD4$^+$ T-cell counts in peripheral blood. Whilst peripheral CD4$^+$ T cells were completely and irreversibly depleted in HVL macaques throughout the infection, they displayed various kinetics in LVL macaques (Fig. 2a). MM397 (Sym LVL) and MM401 (Asym LVL) had very low CD4$^+$ T-cell counts (<150 cells ml^{-1}) at all times at which they were examined after infection, whereas MM399 (Sym LVL) and MM400 (Asym LVL) maintained moderate CD4$^+$ T-cell counts (>300 cells ml^{-1}) throughout the experiment (Fig. 2a).

Naïve CD4$^+$ T cells of MM397 (Sym LVL), MM243 (Asm LVL) and MM401 (Asym LVL) were depleted as early as 4 weeks p.i., whereas those of MM399 (Sym LVL) and MM400 (Asym LVL) remained at moderate levels (Fig. 2b). The HVL macaques were not examined because their peripheral CD4$^+$ T cells were depleted.

In addition to evaluating CD4$^+$ T cells in the blood, we evaluated CD4$^+$ cells in lymphoid and intestinal tissues using CD4 staining. The HVL macaques showed severe depletion of CD4$^+$ cells in all lymphoid tissues and intestine compared with the uninfected macaques (Fig. 2c, d). Interestingly, the CD4$^+$ cell frequencies in the tissues were clearly lower in Sym LVL macaques than in uninfected macaques (Fig. 2c, d). However, the CD4$^+$ cell frequencies in the tissues of Asym LVL macaques were comparable to those in uninfected macaques. These findings indicated that the emergence of diarrhoea and wasting in LVL macaques correlated with the low CD4$^+$ cell frequency in lymphoid tissues and the intestines, but not with the counts of peripheral CD4$^+$ T-cell subsets.

Infected animals exhibit significantly shorter villi

Symptomatic animals (Sym LVL and HVL macaques) exhibited diarrhoea. To examine whether the jejunum of symptomatic animals exhibited the histopathological changes that suggest AIDS-related enteropathy, we measured villous length on haematoxylin and eosin (H&E)-stained samples of jejunum in uninfected and infected macaques. Surprisingly, villous length was significantly

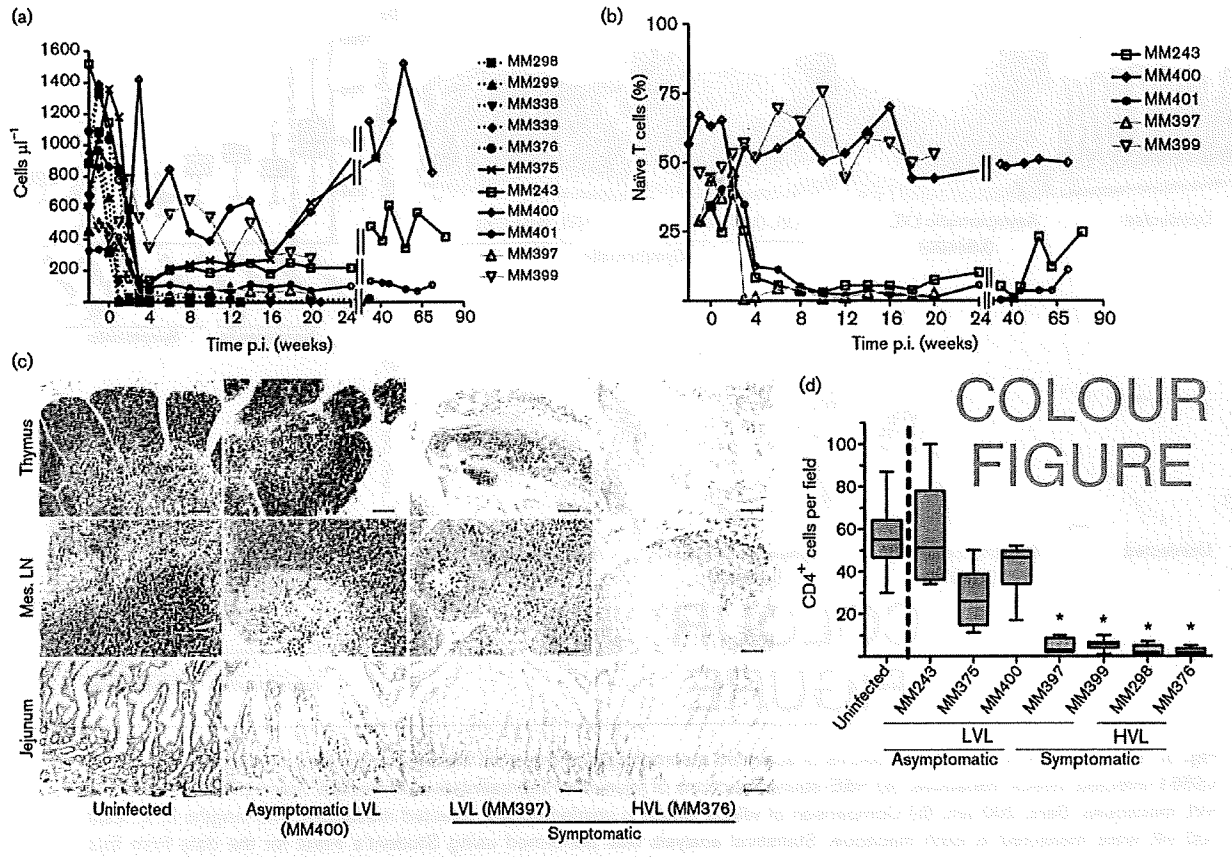

Fig. 2. Counts of circulating CD4$^+$ T-cell subsets and CD4$^+$ cell frequency in lymphoid and intestinal tissues at the time of euthanasia in SHIV-KS661-infected rhesus macaques. Counts of circulating CD4$^+$ T-cell subsets were analysed by flow cytometry and whole-blood counts. (a) Circulating CD4$^+$ T-cell counts. The ID numbers of the macaques are indicated on the figure. (b) Proportion of CD95$^+$ naïve cells in circulating CD4$^+$ T cells of LVL macaques. Solid black lines indicate Asym LVL macaques and solid grey lines indicate Sym LVL macaques. (c) CD4$^+$ cell frequencies in thymus, mesenteric lymph nodes (Mes. LN) and jejunum of representative uninfected, Asym LVL, Sym LVL and HVL macaques. Bars, 100 µm. (d) Quantification of jejunum CD4$^+$ cells in uninfected and infected macaques. The numbers of CD4$^+$ cells were enumerated in at least ten fields of the tissues at a magnification of 200×. Statistical analysis was performed using Student's *t*-test for the data from five uninfected and each infected macaque (*, $P<0.0001$). Data for MM299, MM338, MM339 and MM401 were not available.

shorter in all of the infected animals than in uninfected animals ($P<0.0001$) (Fig. 3a, b). This suggested that SHIV-infected animals develop villous atrophy, irrespective of viral load.

Increased number of activated macrophages in the jejunum of symptomatic animals

Macrophages appeared to be more abundant in H&E-stained jejunal sections in symptomatic animals. This was confirmed by CD68 staining: the frequency of CD68$^+$ macrophages in the jejunum was considerably higher in symptomatic animals than in uninfected animals, but was not significantly different between uninfected animals and Asym LVL macaques (data not shown). Furthermore, CD68$^+$ macrophages in the small intestine of Sym LVL and HVL macaques appeared to be activated because their size was increased. To examine whether the number of activated CD68$^+$ macrophages increased in the small intestine, we double stained for CD68 and Ki67 in the small intestine sections by immunohistochemistry. The frequency of CD68$^+$ Ki67$^+$ macrophages in the jejunum of all symptomatic animals examined was significantly higher than that of uninfected animals ($P<0.0001$) (Fig. 3c, d). This suggested that abnormal activation of intestinal macrophages occurred in symptomatic animals irrespective of viral load.

DISCUSSION

It is important to discuss initially why some SHIV-infected macaques had an HVL at the late stage, whilst others had

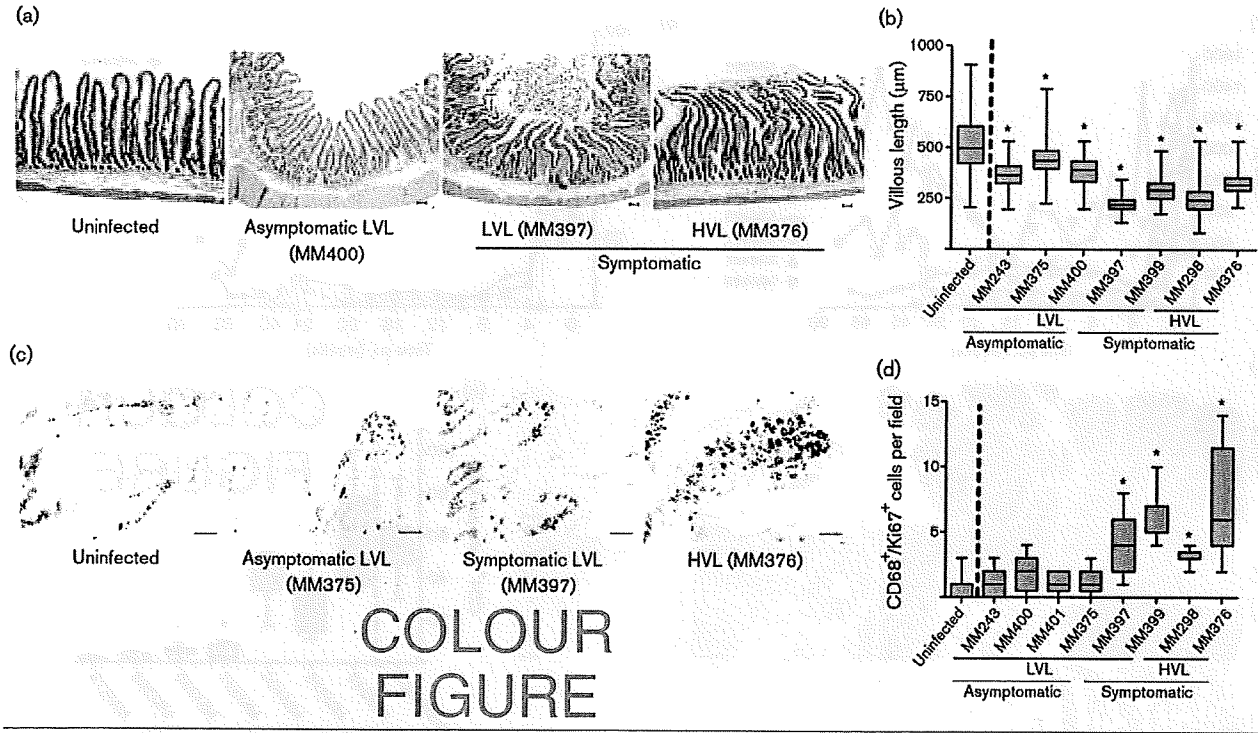

Fig. 3. Villous length in jejunum and counts of activated macrophages in the small intestine at the time of euthanasia in SHIV-KS661-infected rhesus macaques. (a) H&E-stained sections of jejunum of representative uninfected, Asym LVL, Sym LVL and HVL macaques. Bars, 200 μm. (b) Comparison of villous length in uninfected and infected macaques. The lengths of at least 100 villi were measured in each macaque. Statistical analysis was performed using Student's *t*-test for the data from four uninfected and each infected macaque (*, $P<0.0001$). Data for MM299, MM338, MM339 and MM401 were not available. (c) Ki67 and CD68 staining in the small intestine of representative uninfected, Asym LVL, Sym LVL and HVL macaques. Brown staining indicates $Ki67^+$ cells and blue staining indicates $CD68^+$ cells. Bar, 50 μm. (d) Comparison of $CD68^+$ $Ki67^+$ cell counts in uninfected and infected macaques. The numbers of $CD68^+$ $Ki67^+$ cells were enumerated in at least ten fields of the tissues at a magnification of 200×. Statistical analysis was performed using Student's *t*-test for the data from seven uninfected and each infected macaque (*, $P<0.0001$). Data for MM299, MM338 and MM339 were not available.

an LVL. The LVL macaques had much stronger antibody responses than the HVL macaques (Table 1). SHIV-89.6P is easily controlled by the antibody response (Montefiori *et al.*, 1998). SHIV-KS661, which shares its genetic origin with SHIV-89.6P, might be strongly affected by the antibody response. Virus replication during the primary phase clearly occurred later in the intrarectally inoculated macaques than in the intravenously inoculated macaques. Therefore, this delay might contribute to the continuous and strong antibody response in the intrarectally inoculated macaques, consequently resulting in a low viral load in most of the intrarectally inoculated macaques.

The purpose of this study was to elucidate why LVL macaques experience diarrhoea and wasting. A comparison of circulating $CD4^+$ T-cell counts (Fig. 2a) and relative levels of naïve T-cells (Fig. 2b) in LVL macaques did not reveal a substantial difference between Sym LVL (which showed diarrhoea and wasting) and Asym LVL (which were healthy) macaques. The villous length in the intestine also did not affect the level of malignancy of the disease condition, as all infected monkeys showed significant villous atrophy, suggesting a high sensitivity to infection itself. However, Sym LVL and HVL macaques exhibited two findings that Asym LVL macaques did not: (i) $CD4^+$ cell reduction in intestinal and lymphoid tissues (Fig. 2c, d), a hallmark of AIDS; and (ii) abnormal innate immune activation, which was reflected by an increased number of activated macrophages within the intestines (Fig. 3c, d). Ki67 serves as a proliferation marker and proliferation of macrophages may seem unlikely. However, there are some reports about local macrophage proliferation in inflammation sites, indicating the infiltration of activated macrophages associated with tissue damage (Isbel *et al.*, 2001; Norton, 1999). These observations indicated the existence of immunopathological disorders in the intestines not only in HVL macaques but also in Sym LVL macaques.

Many studies have shown positive correlations between the development of AIDS and some characteristic features in

the intestinal tracts of HIV-1-infected humans and pathogenic SIV- or SHIV-infected monkeys: continuous $CD4^+$ T-cell depletion (Brenchley *et al.*, 2004; Ling *et al.*, 2007), abnormal and chronic immune activation (Brenchley *et al.*, 2006; Hazenberg *et al.*, 2003) and enteropathy (Kotler, 2005). Immune activation (as shown by an increased number of intestinal activated macrophages) and intestinal $CD4^+$ cell depletion in Sym LVL macaques strongly suggest the presence of an AIDS-like disease in this subset of animals. Hence, these results suggest that an AIDS-like intestinal disease can occur in LVL macaques despite their low viral load, as well as in HVL macaques.

Some HIV-1-infected patients experience poor recovery of circulating $CD4^+$ T cells, even when their plasma HIV-1 RNA load is suppressed by HAART (Kaufmann *et al.*, 2003; Marchetti *et al.*, 2006; Piketty *et al.*, 1998). These individuals are called immunological non-responders (Marchetti *et al.*, 2006), and have been found to have increased plasma lipopolysaccharide levels, suggesting that bacteria had been translocated from the intestines into the circulation with concomitant activation of T-cell compartments (Marchetti *et al.*, 2006, 2008). Furthermore, some patients who maintain an undetectable or nearly undetectable plasma viral RNA load in the absence of HAART also develop AIDS disease progression (Madec *et al.*, 2005) and have abnormal immune activation and increased plasma lipopolysaccharide levels (Hunt *et al.*, 2008). These observations may indicate that disease progression in a subset of HIV-1-infected individuals is independent of viraemia. Accordingly, the disease progression under conditions of low viral load that we observed in SHIV-KS661-infected macaques can also occur in HIV-1-infected individuals.

Consistent with the fact that intestinal $CD4^+$ cell depletion triggers mucosal immune dysfunction, a notable difference observed between Sym LVL and Asym LVL macaques was the low $CD4^+$ cell frequency in the intestines of the Sym LVL macaques. We propose that the intestinal $CD4^+$ cells in Sym LVL macaques were not able to recover after intestinal $CD4^+$ cell reduction during the early phases of infection. We reported previously that SHIV-KS661 infection of rhesus macaques caused early intestinal $CD4^+$ T-cell depletion (Fukazawa *et al.*, 2008; Miyake *et al.*, 2006). Although we did not examine the macaques during the early phases of infection, the intestinal $CD4^+$ T cells of both Sym LVL and Asym LVL macaques should have been depleted at this time, as even moderately pathogenic SHIV can cause intestinal $CD4^+$ cell reduction during the early phase of infection (Fukazawa *et al.*, 2008). Therefore, the near-normal frequency of intestinal $CD4^+$ cells in Asym LVL macaques would be the result of $CD4^+$ cell recovery after intestinal $CD4^+$ cell reduction during the early phase of infection. In contrast, intestinal $CD4^+$ cells in Sym LVL macaques may be unable to recover, even though virus replication has been controlled. Similarly, intestinal $CD4^+$ cell recovery was found to be important for halting disease progression in SIVmac239-infected rhesus macaques (Ling *et al.*, 2007). Accordingly, one of the important determinants for disease progression in SHIV-KS661-infected macaques may be $CD4^+$ cell recovery in the intestines.

We further hypothesize that this inappropriately low level of $CD4^+$ cells within the intestines of the SHIV-KS661-infected animals (and phenotypically similar humans) is permissive to the excessive activation of resident tissue macrophages. One implication of these studies is that regulatory T-cell subsets of $CD4^+$ cells may be especially vulnerable to this depletion, thus allowing this macrophage activation in view of the well-known role of regulatory T cells in inhibiting innate immune responses (Maloy *et al.*, 2003). This hypothesis will be important to assess in future studies to understand the pathophysiology in the intestines during the chronic phase of HIV-1 infection.

Taken together, the present results suggest that $CD4^+$ cell reduction and enteropathy can occur in SHIV-KS661-infected rhesus macaques even when the viral load is low. The ability or inability to restore intestinal $CD4^+$ cells may be a key factor determining disease progression, irrespective of virus replication levels in the chronic phase of SHIV-KS661 infection. The reason that the recovery of intestinal $CD4^+$ cells is impeded is unknown, although we can speculate on some possibilities such as the co-existence of other infectious microbial agents or impaired T-cell reconstitution caused by damage during thymopoiesis at an early phase of SHIV infection (Motohara *et al.*, 2006). We demonstrated comparable proviral DNA loads in the examined tissues between Sym and Asym LVL macaques, although the $CD4^+$ cell frequencies in the tissues were clearly reduced in Sym LVL macaques. Therefore, the quantity of provirus per CD4 cell in the tissues of Sym LVL macaques is considered to be relatively higher than that of Asym LVL macaques, and low-level replication that may be undetectable in the plasma viral load might be maintained in Sym LVL but not in Asym LVL macaques. Identifying the mechanisms of poor recovery of intestinal $CD4^+$ cells is needed to understand AIDS pathogenesis, because, as stated above, some HIV-1-infected patients have low $CD4^+$ T-cell counts even when viraemia is controlled. One useful approach is comparative and periodical analysis, including cellular immunology data, of the intestinal tract of the same animals from the early to the chronic phases using Sym LVL and Asym LVL macaques in this SHIV infection macaque model.

METHODS

Virus, animals and sample collection. Highly pathogenic SHIV-KS661 is a molecular clone of SHIV-C2/1 (GenBank accession no. AF217181), which was derived through *in vivo* passages of SHIV-89.6 (Shinohara *et al.*, 1999). The virus stock was prepared from the supernatant of virus-infected CEMx174 and M8166 human lymphoid cell lines.

All rhesus macaques used in this study were treated in accordance with the institutional regulations approved by the Committee for

Experimental Use of Non-human Primates in the Institute for Virus Research, Kyoto University, Japan. All macaques were inoculated with 2×10^3 50 % tissue culture infectious dose of SHIV-KS661 measured with CEMx174. The animal ID numbers, infection route and when they were euthanized are provided in Fig. 1(a).

Blood was collected periodically using sodium citrate as an anti-coagulant and examined by flow cytometry and for quantification of plasma viral RNA load. Tissue samples were obtained at the time of euthanasia and were used for quantification of proviral DNA and histopathology.

Determination of plasma viral RNA and proviral DNA loads. The viral loads in plasma and proviral DNA loads in lymphoid and intestinal tissues were determined by quantitative RT-PCR and quantitative PCR, respectively, as described previously (Motohara *et al.*, 2006). DNA samples were extracted directly from frozen tissue sections of each monkey using a DNeasy Tissue kit (Qiagen) according to the manufacturer's protocol.

Determination of antibody titres. Anti-HIV antibody titres were determined using a commercial particle agglutination kit (Serodia-HIV1/2; Fujirebio). Isolated plasma samples were serially diluted and assayed. The end point of the highest dilution giving a positive result was determined as the titre.

Flow cytometry. Flow cytometry was performed as described previously (Motohara *et al.*, 2006). Briefly, $CD4^+$ T cells were analysed by a combination of fluorescein isothiocyanate (FITC)-conjugated anti-monkey CD3 (clone FN-18; BioSource) and phycoerythrin-conjugated anti-human CD4 (clone NU-TH/I; Nichirei), and subsets of naïve and memory $CD4^+$ cells were analysed by a combination of FITC-conjugated anti-human CD95 (clone DX2; BD Pharmingen) and allophycocyanin-conjugated anti-human CD4 (clone L200; BD Pharmingen). $CD95^-$ $CD4^+$ cells were defined as naïve $CD4^+$ T cells and $CD95^+$ $CD4^+$ cells were defined as memory $CD4^+$ T cells. Labelled lymphocytes were examined on a FACSCalibur analyser using CellQuest software (BD Biosciences).

Histology and immunohistochemistry. Tissue samples were fixed in 4 % paraformaldehyde in PBS at 4 °C overnight and embedded in paraffin wax. Sections (4 μm) were dewaxed using xylene, rehydrated through an alcohol gradient, and stained with H&E. The villous length of the jejunum was measured with a micrometer. At least 40 villi from each section were measured.

For immunohistochemistry, sections were rehydrated and processed for 10 min in an autoclave in 10 mM citrate buffer (pH 6.0) to unmask the antigens, sequentially treated with TBS/Tween 20 (TBST) and aqueous hydrogen peroxide, left at 4 °C overnight or at room temperature for 30 min or 1 h for primary antibody reactions, washed with TBST, incubated at room temperature for 1 h with an Envision+ kit (a horseradish peroxidase-labelled anti-mouse immunoglobulin polymer; Dako), visualized using diaminobenzidine (DAB) substrate (Dako) as a chromogen, rinsed in distilled water, counterstained with haematoxylin and analysed by light microscopy (Biozero BZ-8000: Keyence).

For double staining (CD68 and Ki67) of sections, appropriately processed sections were incubated at room temperature for 1 h with unlabelled anti-Ki67 antibody at a dilution of 1:2000, the highly sensitive tyramide amplification step (CSAII; Dako) was performed, the slides were reacted with DAB to visualize the results and incubated with unlabelled anti-CD68 antibody at 4 °C overnight followed by incubation at room temperature for 1 h with Histofine Simple Stain AP (an alkaline phosphatase-labelled anti-mouse immunoglobulin polymer (Nichirei), and the results were visualized with a Blue Alkaline Phosphatase Substrate kit III (Vector Laboratories). Measurements of $CD68^+$ $Ki67^+$ cell counts were performed in ten fields at a magnification of 200 × by light microscopy.

Primary antibodies used in immunohistochemistry were anti-human CD4 (diluted 1:30; clone NCL-CD4; Novacastra Laboratories), anti-SIV Nef (diluted 1:500; FIT Biotech), anti-human CD68 (diluted 1:50; clone KP-1; Dako) and anti-human Ki67 (Ki-S5; Dako).

Statistical analysis. The significance of $CD4^+$ or $CD68^+$ $Ki67^+$ cell frequency measurements and villous length in the jejunum of infected monkeys compared with uninfected monkeys was analysed using an unpaired Student's *t*-test (two-tailed) using GraphPad Prism 4.0E software (Varsity Wave).

ACKNOWLEDGEMENTS

We are grateful to Dr James Raymond for editing the English of this manuscript; to Takahito Kazama, Reii Horiuchi, Noriko Nakajima and Tetsutaro Sata for technical support; to Dr Michael A. Eckhaus for histopathological interpretation; and to Takeshi Kobayashi for critical reading. This work was supported, in part, by Research on HIV/AIDS in Health and Labour Sciences Research Grants from the Ministry of Health, Labour and Welfare, Japan; a Grant-in-Aid for Scientific Research from the Ministry of Education and Science, Japan; a Research Grant for AIDS on Health Sciences focusing on Drug Innovation from the Japan Health Sciences Foundation; and a Program for the Promotion of Fundamental Studies in Health Sciences of the National Institute of Biomedical Innovation (NIBIO) of Japan.

REFERENCES

Anton, P. A., Elliott, J., Poles, M. A., McGowan, I. M., Matud, J., Hultin, L. E., Grovit-Ferbas, K., Mackay, C. R., Chen, I. S. Y. & Giorgi, J. V. (2000). Enhanced levels of functional HIV-1 co-receptors on human mucosal T cells demonstrated using intestinal biopsy tissue. *AIDS* **14**, 1761–1765.

Batman, P. A., Miller, A. R., Forster, S. M., Harris, J. R., Pinching, A. J. & Griffin, G. E. (1989). Jejunal enteropathy associated with human immunodeficiency virus infection: quantitative histology. *J Clin Pathol* **42**, 275–281.

Brenchley, J. M., Schacker, T. W., Ruff, L. E., Price, D. A., Taylor, J. H., Beilman, G. J., Nguyen, P. L., Khoruts, A., Larson, M. & other authors (2004). $CD4^+$ T cell depletion during all stages of HIV disease occurs predominantly in the gastrointestinal tract. *J Exp Med* **200**, 749–759.

Brenchley, J. M., Price, D. A., Schacker, T. W., Asher, T. E., Silvestri, G., Rao, S., Kazzaz, Z., Bornstein, E., Lambotte, O. & other authors (2006). Microbial translocation is a cause of systemic immune activation in chronic HIV infection. *Nat Med* **12**, 1365–1371.

Fackler, O. T., Schafer, M., Schmidt, W., Zippel, T., Heise, W., Schneider, T., Zeitz, M., Riecken, E. O., Mueller-Lantzsch, N. & Ullrich, R. (1998). HIV-1 p24 but not proviral load is increased in the intestinal mucosa compared with the peripheral blood in HIV-infected patients. *AIDS* **12**, 139–146.

Fukazawa, Y., Miyake, A., Ibuki, K., Inaba, K., Saito, N., Motohara, M., Horiuchi, R., Himeno, A., Matsuda, K. & other authors (2008). Small intestine $CD4^+$ T cells are profoundly depleted during acute simian–human immunodeficiency virus infection, regardless of viral pathogenicity. *J Virol* **82**, 6039–6044.

Gibbons, T. & Fuchs, G. J. (2007). Chronic enteropathy: clinical aspects. *Nestle Nutr Workshop Ser Pediatr Program* **59**, 89–101.

Hazenberg, M. D., Otto, S. A., van Benthem, B. H., Roos, M. T., Coutinho, R. A., Lange, J. M., Hamann, D., Prins, M. & Miedema, F.

(2003). Persistent immune activation in HIV-1 infection is associated with progression to AIDS. *AIDS* **17**, 1881–1888.

Hunt, P. W., Brenchley, J., Sinclair, E., McCune, J. M., Roland, M., Page-Shafer, K., Hsue, P., Emu, B., Krone, M. & other authors (2008). Relationship between T cell activation and $CD4^+$ T cell count in HIV-seropositive individuals with undetectable plasma HIV RNA levels in the absence of therapy. *J Infect Dis* **197**, 126–133.

Isbel, N. M., Nikolic-Paterson, D. J., Hill, P. A., Dowling, J. & Atkins, R. C. (2001). Local macrophage proliferation correlates with increased renal M-CSF expression in human glomerulonephritis. *Nephrol Dial Transplant* **16**, 1638–1647.

Kahn, E. (1997). Gastrointestinal manifestations in pediatric AIDS. *Pediatr Pathol Lab Med* **17**, 171–208.

Kaufmann, G. R., Perrin, L., Pantaleo, G., Opravil, M., Furrer, H., Telenti, A., Hirschel, B., Ledergerber, B., Vernazza, P. & other authors (2003). CD4 T-lymphocyte recovery in individuals with advanced HIV-1 infection receiving potent antiretroviral therapy for 4 years: the Swiss HIV Cohort Study. *Arch Intern Med* **163**, 2187–2195.

Kotler, D. P. (2005). HIV infection and the gastrointestinal tract. *AIDS* **19**, 107–117.

Lapenta, C., Boirivant, M., Marini, M., Santini, S. M., Logozzi, M., Viora, M., Belardelli, F. & Fais, S. (1999). Human intestinal lamina propria lymphocytes are naturally permissive to HIV-1 infection. *Eur J Immunol* **29**, 1202–1208.

Ling, B., Veazey, R. S., Hart, M., Lackner, A. A., Kuroda, M., Pahar, B. & Marx, P. A. (2007). Early restoration of mucosal CD4 memory CCR5 T cells in the gut of SIV-infected rhesus predicts long term non-progression. *AIDS* **21**, 2377–2385.

Madec, Y., Boufassa, F., Porter, K. & Meyer, L. (2005). Spontaneous control of viral load and CD4 cell count progression among HIV-1 seroconverters. *AIDS* **19**, 2001–2007.

Maloy, K. J., Salaun, L., Cahill, R., Dougan, G., Saunders, N. J. & Powrie, F. (2003). $CD4^+CD25^+$ T_R cells suppress innate immune pathology through cytokine-dependent mechanisms. *J Exp Med* **197**, 111–119.

Marchetti, G., Gori, A., Casabianca, A., Magnani, M., Franzetti, F., Clerici, M., Perno, C. F., Monforte, A., Galli, M. & Meroni, L. (2006). Comparative analysis of T-cell turnover and homeostatic parameters in HIV-infected patients with discordant immune-virological responses to HAART. *AIDS* **20**, 1727–1736.

Marchetti, G., Bellistri, G. M., Borghi, E., Tincati, C., Ferramosca, S., La Francesca, M., Morace, G., Gori, A. & Monforte, A. D. (2008). Microbial translocation is associated with sustained failure in $CD4^+$ T-cell reconstitution in HIV-infected patients on long-term highly active antiretroviral therapy. *AIDS* **22**, 2035–2038.

Miyake, A., Ibuki, K., Enose, Y., Suzuki, H., Horiuchi, R., Motohara, M., Saito, N., Nakasone, T., Honda, M. & other authors (2006). Rapid dissemination of a pathogenic simian/human immunodeficiency virus to systemic organs and active replication in lymphoid tissues following intrarectal infection. *J Gen Virol* **87**, 1311–1320.

Montefiori, D. C., Reimann, K. A., Wyand, M. S., Manson, K., Lewis, M. G., Collman, R. G., Sodroski, J. G., Bolognesi, D. P. & Letvin, N. L. (1998). Neutralizing antibodies in sera from macaques infected with chimeric simian–human immunodeficiency virus containing the envelope glycoproteins of either a laboratory-adapted variant or a primary isolate of human immunodeficiency virus type 1. *J Virol* **72**, 3427–3431.

Motohara, M., Ibuki, K., Miyake, A., Fukazawa, Y., Inaba, K., Suzuki, H., Masuda, K., Minato, N., Kawamoto, H. & other authors (2006). Impaired T-cell differentiation in the thymus at the early stages of acute pathogenic chimeric simian–human immunodeficiency virus (SHIV) infection in contrast to less pathogenic SHIV infection. *Microbes Infect* **8**, 1539–1549.

Norton, W. T. (1999). Cell reactions following acute brain injury: a review. *Neurochem Res* **24**, 213–218.

Paiardini, M., Frank, I., Pandrea, I., Apetrei, C. & Silvestri, G. (2008). Mucosal immune dysfunction in AIDS pathogenesis. *AIDS Rev* **10**, 36–46.

Piketty, C., Castiel, P., Belec, L., Batisse, D., Si Mohamed, A., Gilquin, J., Gonzalez-Canali, G., Jayle, D., Karmochkine, M. & other authors (1998). Discrepant responses to triple combination antiretroviral therapy in advanced HIV disease. *AIDS* **12**, 745–750.

Sestak, K. (2005). Chronic diarrhea and AIDS: insights into studies with non-human primates. *Curr HIV Res* **3**, 199–205.

Sharpstone, D. & Gazzard, B. (1996). Gastrointestinal manifestations of HIV infection. *Lancet* **348**, 379–383.

Shinohara, K., Sakai, K., Ando, S., Ami, Y., Yoshino, N., Takahashi, E., Someya, K., Suzaki, Y., Nakasone, T. & other authors (1999). A highly pathogenic simian/human immunodeficiency virus with genetic changes in cynomolgus monkey. *J Gen Virol* **80**, 1231–1240.

Smith, P. D., Meng, G., Salazar-Gonzalez, J. F. & Shaw, G. M. (2003). Macrophage HIV-1 infection and the gastrointestinal tract reservoir. *J Leukoc Biol* **74**, 642–649.

Veazey, R. S., DeMaria, M., Chalifoux, L. V., Shvetz, D. E., Pauley, D. R., Knight, H. L., Rosenzweig, M., Johnson, R. P., Desrosiers, R. C. & Lackner, A. A. (1998). Gastrointestinal tract as a major site of $CD4^+$ T cell depletion and viral replication in SIV infection. *Science* **280**, 427–431.

Veazey, R. S., Mansfield, K. G., Tham, I. C., Carville, A. C., Shvetz, D. E., Forand, A. E. & Lackner, A. A. (2000a). Dynamics of CCR5 expression by $CD4^+$ T cells in lymphoid tissues during simian immunodeficiency virus infection. *J Virol* **74**, 11001–11007.

Veazey, R. S., Tham, I. C., Mansfield, K. G., DeMaria, M., Forand, A. E., Shvetz, D. E., Chalifoux, L. V., Sehgal, P. K. & Lackner, A. A. (2000b). Identifying the target cell in primary simian immunodeficiency virus (SIV) infection: highly activated memory $CD4^+$ T cells are rapidly eliminated in early SIV infection in vivo. *J Virol* **74**, 57–64.

Wilcox, C. M. & Saag, M. S. (2008). Gastrointestinal complications of HIV infection: changing priorities in the HAART era. *Gut* **57**, 861–870.

Arch Dermatol Res
DOI 10.1007/s00403-008-0873-y

ORIGINAL PAPER

Administration of Ag85B showed therapeutic effects to Th2-type cytokine-mediated acute phase atopic dermatitis by inducing regulatory T cells

Hitoshi Mori · Keiichi Yamanaka · Kazuhiro Matsuo · Ichiro Kurokawa · Yasuhiro Yasutomi · Hitoshi Mizutani

Received: 5 February 2008 / Revised: 22 May 2008 / Accepted: 20 June 2008

Abstract Increase in the number of patients with atopic dermatitis (AD) has been recently reported. T helper (Th) cells that infiltrate AD skin lesions are Th2-type dominant; reduced exposure to environmental Th1-cytokine-inducing microbes is believed to contribute to the increased number of AD patients. Regulatory type immune responses have been also associated with the occurrence of AD. It has been reported that antigen 85B (Ag85B) purified from mycobacteria is a potent inducer of Th1-type immune response in mice as well as in humans. In this study, we have examined the effect of plasmid DNA encoding Ag85B derived from *Mycobacterium kansasii* on AD skin lesions induced by oxazolone (OX) application. Th2-cytokine mediated mouse AD model with immediate type response followed by a late phase reaction was developed by repeated applications of low-dose OX to sensitized mice. Mice were immunized with plasmid DNA encoding cDNA of Ag85B before OX sensitization or during repeated elicitation phase. Both therapies were associated with significant suppression of immediate type response, clinical appearance, dermal cell infiltration, reduced IL-4 production, and augmented IFN-γ mRNA expression compared to placebo-treated mice. Additionally, increased number of Foxp3$^+$ regulatory T cells were observed in the skin sections in Ag85B treated mice. The results of this study suggest that Ag85B DNA vaccine is a potential therapy for Th2 type dermatitis.

Keywords Atopic dermatitis · Antigen 85B · Regulatory T cell

Abbreviations

AD	Atopic dermatitis
Th	T helper
BCG	*Bacillus Calmette-Güerin*
Treg	Regulatory T cell
Ag85B	Antigen 85B
OX	Oxazolone

Introduction

It is known that acute phase skin lesion in atopic dermatitis (AD) is associated with enhanced secretion of T helper (Th) 2-type cytokines [8]. Increased incidence of atopic disorders has been reported in industrialized countries; according to the hygiene hypothesis, the increase in the incidence of patients may be explained by a better lifestyle and less exposure to environmental microbes [5, 7, 28]. Environmental microbes such as mycobacteria or certain virus may promote Th1-type immune response and thus reducing atopy-associated Th2-type reaction. For instance, the study

H. Mori · K. Yamanaka · I. Kurokawa · H. Mizutani (✉)
Department of Dermatology,
Mie University Graduate School of Medicine,
2-174 Edobashi, Tsu, Mie 514-8507, Japan
e-mail: h-mizuta@clin.medic.mie-u.ac.jp

K. Matsuo
Research and Development Department,
Japan BCG Laboratory, Tokyo, Japan

Y. Yasutomi
Laboratory of Immunoregulation and Vaccine Research,
Tsukuba Primate Research Center,
National Institute of Biomedical Innovation,
Tsukuba, Ibaraki, Japan

Y. Yasutomi
Department of Immunoregulation,
Mie University Graduate School of Medicine,
Tsu, Mie, Japan

carried out in Japanese *Bacillus Calmette-Güerin* (BCG)-vaccinated school children showed that responders to tuberculin had a lower prevalence of atopic disease compared to tuberculin non-responders [28]. BCG-treated mice showed suppression of experimental allergic responses [12]. More recently, it has been shown that microbial stimulation can induce regulatory T (Treg) cells with the ability to suppress both Th1-type and Th2-type inflammation [35]. In the experimental model of pulmonary inflammation, *Mycobacterium vaccae* reduces allergic pulmonary inflammation significantly by increasing the number of Treg cells that secretes IL-10 and TGF-β[37]. These observations indicate that shift from Th2 to Th1 type immune response by mycobacteria may be used for the prevention and treatment of atopic disorders.

The specific antigens eliciting Th1-type immune responses in mycobacteria have not been elucidated so far; a recent study suggested that one of the specific proteins for Th1 development is antigen 85B (Ag85B) [31]. Ag85B is a 30-kDa major protein secreted from all *Mycobacterium* species and that belongs to the Ag85 family[4]. The Ag85B can induce a strong Th1-type immune response in mice as well as in humans [31], and DNA vaccines encoding Ag85B have been reported to protect animals from tuberculosis infection by inducing Th1 response [34, 36]. We have previously reported enhancement of anti-tumor specific CTL response using Ag85B-transfected tumor cells, and by inducing Th1-type immune responses as a vaccine adjuvant [22, 30].

The purpose of the present study was to evaluate the therapeutic efficacy of Ag85B derived from *M. kansasii* in acute phase dermatitis. Repeated applications of hapten such as oxazolone (OX) on BALB/c mice causes delayed type hypersensitivity in the beginning that changes to an immediate-type response in the late phases with elevated IgE production, and deviation of Th cell responses. The skin lesions that appear in late phases are compatible with the clinical findings as well as cytokine profile observed in AD [19, 21]. In all Ag85B-treated AD mice, the immediate type reaction is effectively suppressed and IL-4 is significantly reduced. The results of this study provide evidence for the potential usefulness of Ag85B as a novel approach for the treatment of Th2 type-mediated dermatitis such as AD.

Materials and methods

Animals

Six-week-old BALB/c male mice were purchased from Japan SLC Co. (Shizuoka, Japan) and used at the age of 7 weeks. Animal care was done according to ethical guidelines, and approved by the Institutional Board Committee for Animal Care and Use of Mie University.

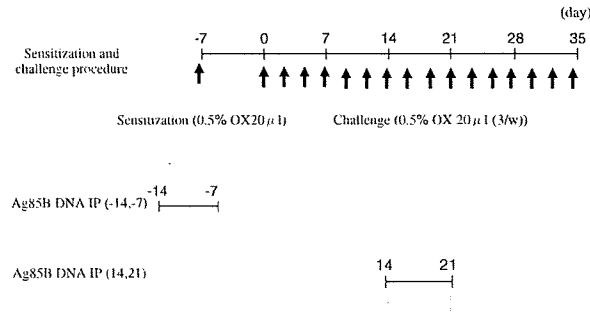

Fig. 1 Model of chronic contact hypersensitivity, and treatment with Ag85B DNA

Sensitization and challenge of animals

Oxazolone was purchased from Sigma (St Louis, MO, USA), and dissolved in acetone/olive oil (1:1). As shown in Fig. 1, mice were initially sensitized by pasting 20 μl of 0.5% OX solution to their left ear 7 days prior to the first challenge (day -7) and then 20 μl of 0.5% OX solution was repeatedly applied on the left ear three times per week from day 0. The ear swelling response was expressed as the difference between before and 30 min after application. The Ag85B expression vector pcDNA-Ag85B of *M. kansasii* open reading frame lacking a signal sequence has been constructed into KpnI–ApaI sites of pcDNA3.1 as described previously [22]. Plasmid DNAs were purified using the Plasmid Mega Kit (Qiagen, Chatsworth, CA, USA). The empty plasmid pcDNA3.1 was used as a control. Plasmid DNAs were diluted with sterilized physiological saline. Hundred micrograms per mouse of plasmid DNA was injected intraperitoneally on day -14, -7 to evaluate prophylactic effects, or on day 14 and 21 for the assessment of therapeutic effects.

Histological analysis

Skin specimens obtained 30 min after the final challenge were fixed in 10% buffered neutral formaldehyde and embedded in paraffin. Sections prepared of 7 μm thickness were stained with hematoxylin and eosin (H&E), or truidine blue.

Immunohistochemistry

The left ear was sacrificed on day 35, and was embedded in Tissue-Tek OCT compound (Miles, Elkhart, USA), frozen in liquid nitrogen, and cut with a cryostat into 7 μm-thick sections. The tissue preparations were then incubated with

primary antibodies specific for Foxp3 (eBioscience, San Diego) overnight, followed by the additional incubation with Alexa Fluor 633 conjugated secondary antibodies (Molecular Probes, Eugene, OR, USA) for 30 min at room temperature. Sections were examined under Fluoview FV1000 laser scanning confocal microscopy (Olympus, Tokyo, Japan). The numbers of $Foxp3^+$ cells were counted in high power fields; five randomly chosen fields were evaluated.

Analysis of cytokine mRNA expression in mouse ears

At 6 h after the final challenge, the left ear skin was sampled. The specimen was homogenized and mRNA was extracted using Isogen (Nippon Gene, Tokyo, Japan) according to the manufacture's instruction; 1 ml of homogenate was vigorously mixed with 200 μl of chloroform, and then centrifuged at 15,000 rpm for 15 min at 4°C. Aqueous phase was separated and mixed with 0.5 ml of 2-propanol (Nacalai Tesque, Kyoto, Japan) to precipitate RNA. After centrifugation, the precipitate was washed with 1 ml of 75% ethanol (Nacalai Tesque) and dried up. RNA was suspended in 50 μl of RNase-free water, the concentration was calculated based on the absorbance at 260 nm, and the quality was confirmed by electrophoresis. cDNA was synthesized from 10 μg of mRNA using archive kit (ABI, Foster City, CA, USA) according to the manufacturer's protocol.

Cytokine mRNA expression in skin

Real time quantitative reverse transcription-polymerase chain reaction (RT-PCR) was performed to measure transcriptional activity in the skin lesions. A 25-μl reaction mixture containing 1 μg total of cDNA, 900 nmol of each primer, and 250 nmol of TaqMan probe were mixed with 12.5 μl of TaqMan Master Mix (ABI, Foster City, CA, USA). The following primers and probes were used for the PCR reactions: mouse IL-4; forward: 5′-ACAGGAGAA GGGACGCCAT-3′, reverse: 5′-GAAGCCCTACAGAC GAGCTCA-3′, probe: 5′-TCCTCACAGCAACGAAGAA CACCACA-3′-TAMRA, IFN-γ; forward: 5′-TCAAGTG GCATAGATGTGGAAGAA-3′, reverse: 5′-TGGCTCT GCAGGATTTTCATG-3′, probe: 5′-TCACCATCCTTTT GCCAGTTCCTCCAG-3′-TAMRA, IL-10; forward: 5′-G GTTGCCAAGCCTTATCGGA-3′, reverse: 5′-ACCTGCT CCACTGCCTTGCT, probe: 5′-TGAGGCGCTGTCGTC ATCGATTTCTCCC-3′-TAMRA, TGF-β; forward: 5′-TG ACGTCACTGGAGTTGTACGG-3′, reverse: 5′-GGTTC ATGTCATGGATGGTGC-3′, probe: 5′-TTCAGCGCTC ACTGCTCTTGTGACAG-3′-TAMRA, β-actin; forward: 5′-AGAGGGAAATCGTGCGTGAC-3′, reverse: 5′-CAA TAGTGATGACCTGGCCGT-3′, probe: 5′-CACTGCCG CATCCTCTTCCTCCC-3′-TAMRA [25]. PCR was performed under the following conditions: 95°C for 10 min, then 40 cycles of 95°C for 15 s, 60°C for 1 min were carried out. Fluorescence data were collected during each annealing-extension step and analyzed by using ABI Prism SDS software version 1.9.1. All samples were normalized for to the β-actin mRNA content.

Measurement of serum IgE

Blood was collected under anesthesia 6 h after the last challenge. Serum IgE levels were determined by a sandwich enzyme-linked immunosorbent assay (BD PharMingen, CA, USA) according to the manufacturer's instructions. Optical density of each well was determined by using a microplate reader (Multiscan JX) (Thermo Electron, Yokohama, Japan). Standard curve was prepared using mouse anti-TNP IgE standard (BD PharMingen, CA, USA) diluted with PBS containing 10% FCS.

Statistical analysis

Differences in ear swelling and serum IgE levels were analyzed by the Kruskal–Wallis test. $P < 0.05$ was taken as significant.

Results

Effect of Ag85B on skin inflammation

We first examined whether Ag85B could modulate ear-swelling reaction in a mouse model of OX-induced AD like skin lesions. Repeated applications of OX cause Th2-mediated immediate type response. Ear swelling was measured with thickness gauge calipers before and 30 min after OX challenge on the pinna of the ear on day 32. In both prophylactic and therapeutic models, the administration of Ag85B significantly suppressed swelling compared to placebo-treated controls (Fig. 2a). The OX-challenged placebo-treated mice showed severe skin inflammation, however administration of Ag85B DNA reduced atopic inflammatory reactions (Fig. 2b).

Histological analysis

Histological examination in OX-challenged mice showed epidermal hyperplasia and strong intraepidermal and intradermal inflammatory cell infiltration including mononuclear cells, neutrophils, and granular cells (Fig. 3a). Both prophylactic and therapeutic administration of Ag85B DNA clearly reduced inflammatory cell infiltration and epidermal thickness. Skin sections stained with truidine blue showed decreased mast cell infiltration in Ag85B-treated mice (Fig. 3b).

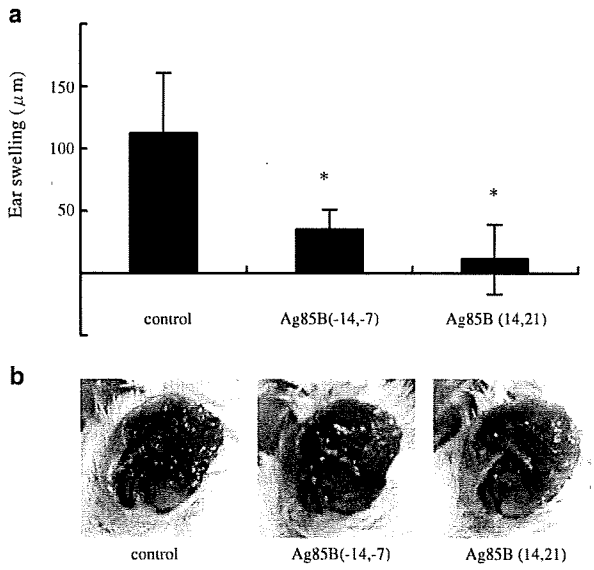

Fig. 2 **a** OX-induced ear swelling. The ear swelling response was expressed as the difference between ear thickness before and 30 min after each application on day 32. The columns and error bars represent mean ± SEM. $*P < 0.05$. Swelling was suppressed significantly in Ag85B-treated mice compared with those in placebo-treated mice. **b** Clinical features of ear skin on day 35. The OX-challenged mice showed severe skin eruption, however administration of the Ag85B DNA in both prophylactic and therapeutic models clearly reduced atopic inflammatory reactions in OX-sensitized mice

Ag85B treatment shifted the Th1/Th2 balance toward Th1

IFN-γ and IL-12 shift the Th1/Th2 balance toward Th1 condition; while IL-4 and IL-5 are key cytokines in Th2 response [24, 29]. To clarify the type of immune response in skin lesions after treatment with Ag85B, we analyzed the mRNA expression levels of IL-4 and IFN-γ by real time quantitative RT-PCR. The results were normalized to the β-actin mRNA content. As shown in Fig. 4, the expression of IL-4 mRNA was reduced in Ag85B-treated mice in both prophylactic and therapeutic models. On the contrary, the expression of IFN-γ was enhanced in Ag85B-treated mice. These results suggest that the application of Ag85B shifts the immune response toward Th1-predominace.

Total serum IgE levels

Atopic dermatitis is characterized by elevated IgE levels. Repeated applications of OX cause a gradual elevation of antigen-specific IgE level. We analyzed the degrees of IgE levels in sera collected from experimental mice. Administration of Ag85B significantly reduced the serum levels of IgE (Fig. 5).

Ag85B treatment induces regulatory T cells

TGF-β and IL-10 are important regulatory cytokines produced by Treg [11]. To investigate the mechanisms of the therapeutic effectiveness of Ag85B, we examined the mRNA levels of TGF-β and IL-10. As shown in Fig. 6a, TGF-β and IL-10 were significantly increased in Ag85B-treated mice in both prophylactic and therapeutic models. And then, we next looked at the induction of Treg in the inflamed skin. Naturally occurring $CD4^+CD25^+$ Treg are characterized by the expression of Foxp3 [10, 27]. Skin sections were stained with anti-Foxp3 mAb, and examined with a fluorescent microscope. As shown in Fig. 6b, $Foxp3^+$ cells were increased in the Ag85B-treated mice.

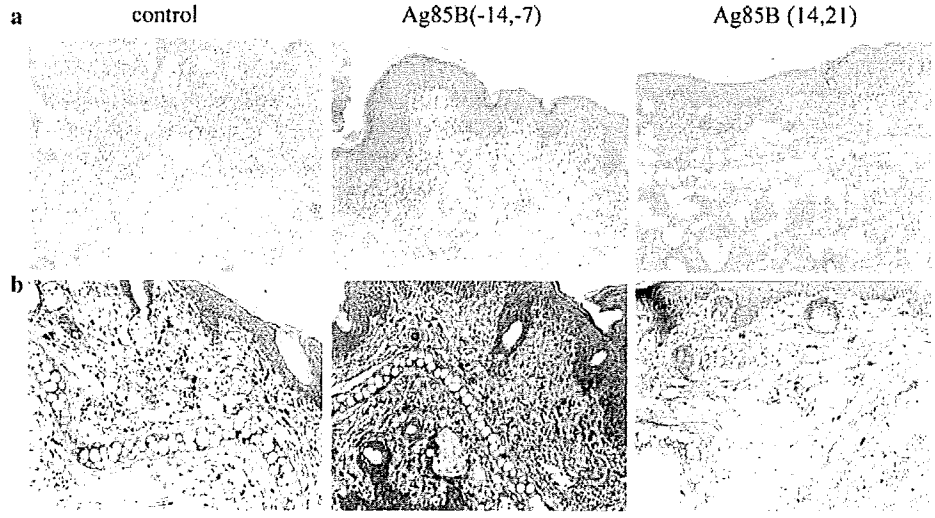

Fig. 3 Histopathological features of skin lesions. Skin was taken on day 35, paraffin embedded sections were stained with **a** hematoxylin and eosin or **b** truidine blue. OX-challenged mice showed epidermal hyperplasia along with strong intradermal inflammatory cell infiltration; whereas Ag85B DNA significantly reduced the inflammatory changes

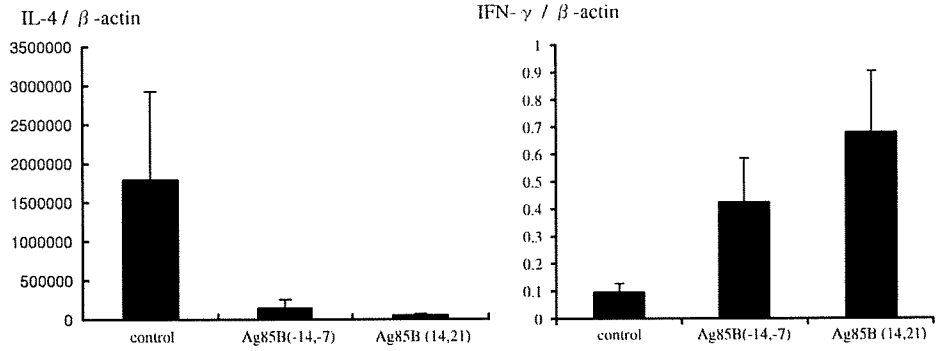

Fig. 4 mRNA expression in the ear on day 35. In order to clarify the expression of cytokine mRNA, quantitative PCR was performed by using specific primers and probes for IL-4 and IFN-γ. The expression of IL-4 mRNA was reduced in Ag85B-treated mice compared with placebo-treated mice. On the other hand, mRNA expression of IFN-γ was significantly increased in Ag85B mice

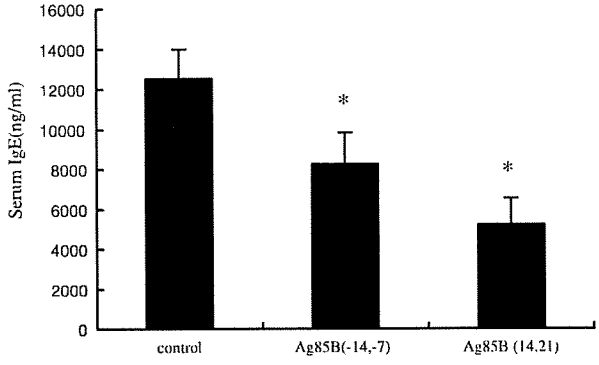

Fig. 5 Serum IgE concentrations. Serum IgE levels were measured on day 35 in control, Ag85B DNA IP (−14, −7), or Ag85B DNA IP (14, 21) mice. The columns and error bars represent mean ± SEM. $^*P < 0.05$. Administration of Ag85B reduced IgE level

Discussion

Human immune system responds to exogenous microorganisms for self-protection. These responses lead to Th1 and/ or Th2 type cytokine secretion depending on the nature of stimuli. AD is a chronic dermatitis characterized by a Th2-type immune responses that causes elevation of IgE. On the other hand, some bacterial infections including *Mycobacterium* species elicits strong Th1-type responses. Inducers of Th1 type immune response may be used as immuno-modulator having therapeutic effects against allergic disease elicited by Th2-type immune responses. Mycobacteria may affect atopic disorders by correction of the immune response from Th2 to Th1. Erb et al. reported that *M. bovis* (BCG) suppresses airway eosinophilia and associated local IL-5 production by inducing Th1-mediated response [9]. Furthermore, recent studies suggested that mycobacteria induce not only Th cells providing Th1 type immune responses but also Treg cells. In an animal model of allergy, the immunomodulatory effects of *M. vaccae* was found to be mediated by allergen-specific regulatory T lymphocytes [37], and oral administration of *M. vaccae* inhibited pulmonary allergic inflammation by induction of IL-10 [14].

Alive BCG vaccination has been used for prevention of tuberculosis. The use of *Mycobacterium* for immunomodulation requires repeated exposures to the immune system. However, repeated alive BCG vaccination is contraindicated. For human therapeutic application, it needs intradermal or intramuscular injection for vaccination. Unfortunately, cutaneous vaccination with *Mycobacterium* species commonly produces granulomatous formation leading to recalcitrant ulcers. We need to develop Th1 type immunomodulating system that induces no granulomatous reaction, if species of mycobacteria are tried to use for human. The Ag85B protein is a main component of the cell wall of mycobacteria such as *M. tuberculosis and M. kansasii* [4]; this Ag85B is known as a strong Th1 inducer in vitro [17, 18]. Experiments using plasmid DNA encoding Ag85B has been previously reported. This Ag85B is able to protect against *M. tuberculosis* even in Balb/c mice [33]. Intraperitoneal administration of Ag85B DNA inhibits granulomatous changes or adhesive reaction of intraperitoneal organs in mice (data not shown). As a preliminary study, Ag85B DNA was intradermally injected in the skin of mice skin. No ulcerative changes were observed in vaccinated areas of the skin (data not shown).

In our present study, we evaluated the efficacy of DNA encoding Ag85B for inducing Th1- and Treg-type immune response in OX-induced acute phase dermatitis. Repeated applications of OX in mice ears caused Th2-type dominant dermatitis, which mimic most of the characteristic features of AD [16, 19, 20, 32]. We first investigated whether the application of Ag85B corrects the immune response from a type Th2 one to a type Th1 response. Our results showed that Ag85B successfully ameliorates Th2-cytokine dominant immediate type reaction in the skin lesions in both prophylactic and therapeutic models of the disease. In Ag85B-treated AD skin lesion, the ear swelling was significantly reduced compared to placebo-treated animals. Administration of Ag85B DNA suppressed histological abnormalities caused by atopic inflammations such as inflammatory cell infiltration, epidermal hyperplasia, and severe edema. The presence of mast cells in the skin lesion is closely associated with Th2-type dermatitis; the number of mast cells was

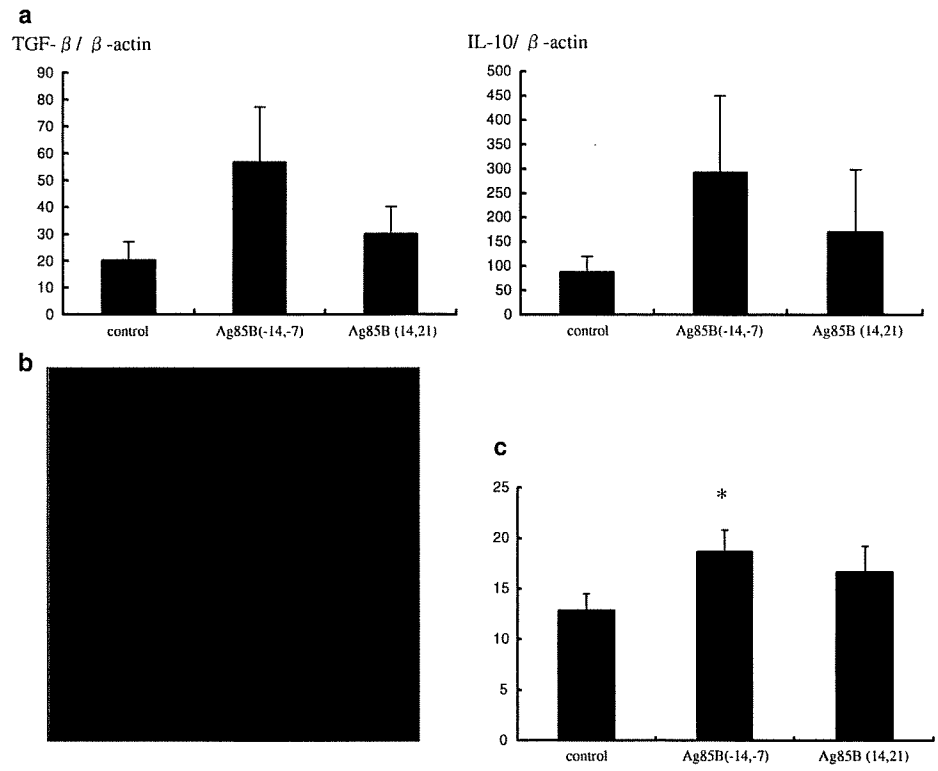

Fig. 6 **a** mRNA expression in the ear on day 35. Quantitative PCR was performed by using specific primers and probes for IL-10 and TGF-β. Both TGF-β and IL-10 were increased in the Ag85B-treated mice. **b** $Foxp3^+$ cells were clearly observed with confocal microscopy. **c** The number of $Foxp3^+$ cells per HPF was counted in five nonconsecutive fields, and $Foxp3^+$ cells were found to be increased in Ag85B-treated mice

increased in OX-treated control animals as expected; however, the number of mast cells was decreased in Ag85B-treated mice compared with controls. Enhancement of the expression of IFN-γ mRNA was significant in Ag85B-treated AD mice compared with placebo-treated animals. The expression of IL-4 mRNA were suppressed in Ag85B-treated mice compared to placebo-treated controls (Fig. 4). In addition, serum IgE levels were significantly suppressed in Ag85B treated mice compared with placebo-treated mice. These finding demonstrates that administration of Ag85B DNA significantly inhibited the development of Th2-cytokine dominant atopic inflammation by inducing Th1-type immune response.

We also examined the potential of Ag85B to induce Treg cell responses. TGF-β and IL-10 have been described as critical regulatory cytokines produced by Treg [11]. Heat-killed *M. vaccae* induces regulatory T cells that secrete IL-10 and TGF-β [37]. *M. vaccae* also induces a population of $CD11^+$ cells characterized by an increased expression of regulatory cytokines including IL-10 and TGF-β[1]. Treg cells are developed mainly in the presence of IL-10 and TGF-β [13]. More recently, Inoue and Aramaki reported that topical application of CpG-Oligodeoxynucleotides induces $Foxp3^+$ Treg in skin lesions of AD model mice in association with elevation of TGF-β[15]. Depletion of $CD4^+CD25^+$Treg from the peripheral blood of healthy individuals enhances proliferation of Th2 in response to various allergens [6, 23]. The mechanisms of the suppressive activity of Treg depend on cell-to-cell contact, and there is evidence for the involvement of IL-10 and TGF-β[2, 3, 26]. In this study, we have shown elevated expression of TGF-β and IL-10 in Ag85B-treated mice (Fig. 6a), and $Foxp3^+$ Treg was increased in the Ag85B-treated skin (Fig. 6b). We assume that the therapeutics capability of Ag85B is related to the induction of $Foxp3^+$Treg and Th1-type immune response.

In brief, in this study we have shown the usefulness of plasmid DNA of Ag85B for the amelioration of Th1/Th2 imbalance and for the generation of Treg cells. The observations suggest that Ag85B may be useful for the prevention and treatment of atopic disorders.

Acknowledgments This work was supported in part by Health Science Research Grants from the Ministry of Health, Labor and Welfare of Japan and the Ministry of Education, Culture, Sports, Science and Technology of Japan, Grants-in-Aid for Scientific Research and Grants-in-Aid for Core Research Evolutional Science and Technology.

Conflicts of interest statement None.

References

1. Adams VC, Hunt JR, Martinelli R, Palmer R, Rook GA, Brunet LR (2004) *Mycobacterium vaccae* induces a population of pulmonary CD11c+ cells with regulatory potential in allergic mice. Eur J Immunol 34:631–638

2. Akdis M, Verhagen J, Taylor A, Karamloo F, Karagiannidis C, Crameri R, Thunberg S, Deniz G, Valenta R, Fiebig H, Kegel C, Disch R, Schmidt-Weber CB, Blaser K, Akdis CA (2004) Immune responses in healthy and allergic individuals are characterized by a fine balance between allergen-specific T regulatory 1 and T helper 2 cells. J Exp Med 199:1567–1575
3. Asseman C, Mauze S, Leach MW, Coffman RL, Powrie F (1999) An essential role for interleukin 10 in the function of regulatory T cells that inhibit intestinal inflammation. J Exp Med 190:995–1004
4. Belisle JT, Vissa VD, Sievert T, Takayama K, Brennan PJ, Besra GS (1997) Role of the major antigen of *Mycobacterium tuberculosis* in cell wall biogenesis. Science 276:1420–1422
5. Burney PG, Chinn S, Rona RJ (1990) Has the prevalence of asthma increased in children? Evidence from the national study of health and growth 1973–86. BMJ 300:1306–1310
6. Cavani A, Nasorri F, Ottaviani C, Sebastiani S, De Pita O, Girolomoni G (2003) Human CD25+ regulatory T cells maintain immune tolerance to nickel in healthy, nonallergic individuals. J Immunol 171:5760–5768
7. Cookson WO, Moffatt MF (1997) Asthma: an epidemic in the absence of infection? Science 275:41–42
8. Del Prete G (1992) Human Th1 and Th2 lymphocytes: their role in the pathophysiology of atopy. Allergy 47:450–455
9. Erb KJ, Holloway JW, Sobeck A, Moll H, Le Gros G (1998) Infection of mice with *Mycobacterium bovis*-Bacillus Calmette-Guerin (BCG) suppresses allergen-induced airway eosinophilia. J Exp Med 187:561–569
10. Fontenot JD, Gavin MA, Rudensky AY (2003) Foxp3 programs the development and function of CD4+CD25+ regulatory T cells. Nat Immunol 4:330–336
11. Groux H, O'Garra A, Bigler M, Rouleau M, Antonenko S, de Vries JE, Roncarolo MG (1997) A CD4+ T-cell subset inhibits antigen-specific T-cell responses and prevents colitis. Nature 389:737–742
12. Herz U, Gerhold K, Gruber C, Braun A, Wahn U, Renz H, Paul K (1998) BCG infection suppresses allergic sensitization and development of increased airway reactivity in an animal model. J Allergy Clin Immunol 102:867–874
13. Horwitz DA, Zheng SG, Gray JD (2003) The role of the combination of IL-2 and TGF-beta or IL-10 in the generation and function of CD4+ CD25+ and CD8+ regulatory T cell subsets. J Leukoc Biol 74:471–478
14. Hunt JR, Martinelli R, Adams VC, Rook GA, Brunet LR (2005) Intragastric administration of *Mycobacterium vaccae* inhibits severe pulmonary allergic inflammation in a mouse model. Clin Exp Allergy 35:685–690
15. Inoue J, Aramaki Y (2007) Suppression of skin lesions by transdermal application of CpG-oligodeoxynucleotides in NC/Nga mice, a model of human atopic dermatitis. J Immunol 178:584–591
16. Inoue Y, Isobe M, Shiohara T, Goto Y, Hayashi H (2002) Protective and curative effects of topically applied CX-659S, a novel diaminouracil derivative, on chronic picryl chloride-induced contact hypersensitivity responses. Br J Dermatol 147:675–682
17. Kariyone A, Higuchi K, Yamamoto S, Nagasaka-Kametaka A, Harada M, Takahashi A, Harada N, Ogasawara K, Takatsu K (1999) Identification of amino acid residues of the T-cell epitope of *Mycobacterium tuberculosis* alpha antigen critical for Vbeta11(+) Th1 cells. Infect Immun 67:4312–4319
18. Kariyone A, Tamura T, Kano H, Iwakura Y, Takeda K, Akira S, Takatsu K (2003) Immunogenicity of Peptide-25 of Ag85B in Th1 development: role of IFN-gamma. Int Immunol 15:1183–1194
19. Kitagaki H, Fujisawa S, Watanabe K, Hayakawa K, Shiohara T (1995) Immediate-type hypersensitivity response followed by a late reaction is induced by repeated epicutaneous application of contact sensitizing agents in mice. J Invest Dermatol 105:749–755
20. Kitagaki H, Ono N, Hayakawa K, Kitazawa T, Watanabe K, Shiohara T (1997) Repeated elicitation of contact hypersensitivity induces a shift in cutaneous cytokine milieu from a T helper cell type 1 to a T helper cell type 2 profile. J Immunol 159:2484–2491
21. Kitagaki H, Kimishima M, Teraki Y, Hayakawa J, Hayakawa K, Fujisawa S, Shiohara T (1999) Distinct in vivo and in vitro cytokine profiles of draining lymph node cells in acute and chronic phases of contact hypersensitivity: importance of a type 2 cytokine-rich cutaneous milieu for the development of an early-type response in the chronic phase. J Immunol 163:1265–1273
22. Kuromatsu I, Matsuo K, Takamura S, Kim G, Takebe Y, Kawamura J, Yasutomi Y (2001) Induction of effective antitumor immune responses in a mouse bladder tumor model by using DNA of an alpha antigen from mycobacteria. Cancer Gene Ther 8:483–490
23. Ling EM, Smith T, Nguyen XD, Pridgeon C, Dallman M, Arbery J, Carr VA, Robinson DS (2004) Relation of CD4+CD25+ regulatory T-cell suppression of allergen-driven T-cell activation to atopic status and expression of allergic disease. Lancet 363:608–615
24. McKnight AJ, Zimmer GJ, Fogelman I, Wolf SF, Abbas AK (1994) Effects of IL-12 on helper T cell-dependent immune responses in vivo. J Immunol 152:2172–2179
25. Overbergh L, Valckx D, Waer M, Mathieu C (1999) Quantification of murine cytokine mRNAs using real time quantitative reverse transcriptase PCR. Cytokine 11:305–312
26. Powrie F, Carlino J, Leach MW, Mauze S, Coffman RL (1996) A critical role for transforming growth factor-beta but not interleukin 4 in the suppression of T helper type 1-mediated colitis by CD45RB(low) CD4+ T cells. J Exp Med 183:2669–2674
27. Sakaguchi S, Sakaguchi N, Shimizu J, Yamazaki S, Sakihama T, Itoh M, Kuniyasu Y, Nomura T, Toda M, Takahashi T (2001) Immunologic tolerance maintained by CD25+ CD4+ regulatory T cells: their common role in controlling autoimmunity, tumor immunity, and transplantation tolerance. Immunol Rev 182:18–32
28. Shirakawa T, Enomoto T, Shimazu S, Hopkin JM (1997) The inverse association between tuberculin responses and atopic disorder. Science 275:77–79
29. Swain SL, Weinberg AD, English M, Huston G (1990) IL-4 directs the development of Th2-like helper effectors. J Immunol 145:3796–3806
30. Takamura S, Matsuo K, Takebe Y, Yasutomi Y (2005) Ag85B of mycobacteria elicits effective CTL responses through activation of robust Th1 immunity as a novel adjuvant in DNA vaccine. J Immunol 175:2541–2547
31. Takatsu K, Kariyone A (2003) The immunogenic peptide for Th1 development. Int Immunopharmacol 3:783–800
32. Tamura T, Matsubara M, Hasegawa K, Ohmori K, Karasawa A (2005) Olopatadine hydrochloride suppresses the rebound phenomenon after discontinuation of treatment with a topical steroid in mice with chronic contact hypersensitivity. Clin Exp Allergy 35:97–103
33. Teixeira FM, Teixeira HC, Ferreira AP, Rodrigues MF, Azevedo V, Macedo GC, Oliveira SC (2006) DNA vaccine using *Mycobacterium bovis* Ag85B antigen induces partial protection against experimental infection in BALB/c mice. Clin Vaccine Immunol 13:930–935
34. Ulmer JB, Montgomery DL, Tang A, Zhu L, Deck RR, DeWitt C, Denis O, Orme I, Content J, Huygen K (1998) DNA vaccines against tuberculosis. Novartis Found Symp 217:239–246 discussion 246–253
35. Yazdanbakhsh M, Kremsner PG, van Ree R (2002) Allergy, parasites, and the hygiene hypothesis. Science 296:490–494
36. Zhu D, Jiang S, Luo X (2005) Therapeutic effects of Ag85B and MPT64 DNA vaccines in a murine model of *Mycobacterium tuberculosis* infection. Vaccine 23:4619–4624
37. Zuany-Amorim C, Sawicka E, Manlius C, Le Moine A, Brunet LR, Kemeny DM, Bowen G, Rook G, Walker C (2002) Suppression of airway eosinophilia by killed *Mycobacterium vaccae*-induced allergen-specific regulatory T-cells. Nat Med 8:625–629

J. Comp. Path. 2009, Vol. 140, 212–216

Available online at www.sciencedirect.com

ScienceDirect

ELSEVIER
www.elsevier.com/locate/jcpa

SHORT PAPER

Acute Megakaryocytic Leukaemia (AMKL)-like Disease in a Cynomolgus Monkey (*Macaca fascicularis*)

S. Okabayash*,†, C. Ohno* and Y. Yasutomi†

* *The Corporation for Production and Research of Laboratory Primates and* † *Tsukuba Primate Research Center, National Institute of Biomedical Innovation, Hachimandai 1-1, Tsukuba-shi, Ibaraki 305-0843, Japan*

Summary

A 5-year-old male cynomolgus monkey (*Macaca fascicularis*) with a clinical history of bleeding tendency, severe anaemia, thrombocytopenia and elevated serum concentration of liver-related enzymes was examined *post mortem*. Ecchymotic haemorrhages were present on the left eyelid and forehead. The liver, kidney and spleen were markedly enlarged and the kidneys had capsular petechiae. Microscopically, numerous atypical cells resembling myeloid cells were observed in the bone marrow, and myelofibrosis was present. Atypical cells were also present in the blood vessels of the liver, kidney, spleen, lymph nodes, lung, heart, bladder, adrenal gland and brain. Some neoplastic cells had oval or pleomorphic macronuclei and others were multinucleated. Immunohistochemically, the majority of the neoplastic cells had granular cytoplasmic expression of the megakaryocyte-associated antigens Von Willebrand Factor and CD61-IIIa, but were negative for myeloperoxidase. A diagnosis of acute megakaryocytic leukaemia (AMKL)-like disease was made. This would appear to be the first report of AMKL-like disease in non-human primates. This monkey was infected with simian retrovirus type D and it is possible that this viral infection was associated with the development of neoplasia.

Keywords: acute megakaryocytic leukaemia; cynomolgus monkey; immunohistochemistry; simian retrovirus type D

Haematological malignancy has been infrequently documented in monkeys infected by the simian immunodeficiency virus (SIV) (Fortgang *et al.*, 2000). Simian T-cell leukaemia virus (STLV) is also linked to the development of simian T-cell malignancies that closely resemble human T-lymphotropic virus (HTLV) associated leukaemia and lymphoma (Hubbard *et al.*, 1993). Furthermore, simian retrovirus type D (SRV/D) is a common cause of simian acquired immunodeficiency syndrome (SAIDS), a fatal immunosuppressive disease of macaques. SRV/D-infected monkeys may develop lymphadenopathy, splenomegaly, anaemia, bone marrow hyperplasia, lymphoid depletion, neutropenia, weight loss, diarrhoea or malignant neoplasia (Guzman *et al.*, 1999). Although a number of clinical and pathological studies have described lymphoma in non-human primates (Hubbard *et al.*, 1993; Paramastri *et al.*, 2002), there are no reports of myeloid leukaemia in these animals. The present report describes the first case of acute megakaryocytic leukaemia (AMKL)-like disease in a non-human primate.

A 5-year-old male cynomolgus monkey (*Macaca fascicularis*) was housed in the Tsukuba Primate Research Center (TPRC) in an individual cage and maintained according to the National Institute of Biomedical Innovation rules and guidelines for experimental animal welfare. On routine haematological examination, the animal was found to have mild anaemia (red blood cells [RBC] 4.28×10^{12}/l; reference range $5.55–6.63 \times 10^{12}$/l; haemoglobin [Hb] 99 g/l; reference range 105–125 g/l; haematocrit [HCT] 32.7%; reference range 35.4–41.4%) and severe thrombocytopenia (platelets [PLT] 27×10^9/l; reference range $195–339 \times 10^9$/l). The number of white blood cells (WBC) was normal (6.9×10^9/l; reference

Correspondence to: S. Okabayash (e-mail: okarin@primate.or.jp).

0021-9975/$ - see front matter
doi:10.1016/j.jcpa.2008.11.007

range 4.2–9.2 × 10^9/l). Although the animal care staff regularly monitored the health of the animal, at this time no clinical signs were observed. Repeat haematological examinations were performed one and four weeks later, but there was no progression of the anaemia and thrombocytopenia was not present on these occasions. The monkey continued to have normal appetite, faeces and activity.

Three months after the initial haematological examination a spot of blood was detected under the monkey's cage. At this time the animal displayed clinical signs including emaciation, pallor of mucous membranes and haemorrhage on the cutaneous side of one eyelid. Haematological examination revealed severe anaemia (RBC 1.66 × 10^{12}/l, Hb 39 g/l, HCT 13.3%) and thrombocytopenia (PLT 28 × 10^9/l). The WBC count was normal (4.1 × 10^9/l). Serum biochemical examination revealed elevation in the concentration of aspartate aminotransferase (AST, 176 U/l; reference range 31–47 U/l); alanine aminotransferase (ALT, 303 U/l; reference range 21–65 U/l); lactate dehydrogenase (LDH, 7660 U/l; reference range 292–975 U/l), and C reactive protein (CRP, 12.8 mg/l; reference range 0.3–1.7 mg/l).

Cynomolgus monkeys in the TPRC breeding colony are SIV and STLV negative, but most are infected by SRV/D (Hara *et al.*, 2005). The animal described here was seronegative for SRV/D antibody by western blotting, but tested positive by polymerase chain reaction (PCR) for the detection of virus genetic material, consistent with current viraemia. On the basis of the clinical and laboratory data, haematological malignancy was suspected.

The monkey was deeply anaesthetized with a lethal dose of pentobarbital and necropsy examination was performed. Ecchymoses were noted on the left eyelid and forehead. The liver was markedly enlarged and the gallbladder was distended. The kidneys were enlarged, pale red-brown in colour and had capsular petechiation. The spleen was also enlarged, but there were no distinct lymphoid follicles on the cut surface. A dark red nodule (1 cm diameter) was present within each of the inferior lobes of the lung. The femoral bone marrow had a brownish-red appearance.

Tissues were fixed in 10% neutral buffered formalin, processed routinely and embedded in paraffin wax. Sections (3 μm) were stained with haematoxylin and eosin (HE), periodic acid-Schiff (PAS) and Masson's trichrome stains. Microscopically, many atypical cells resembling myeloid cells were observed in the bone marrow and the blood vessels of the liver, kidney, spleen, lymph nodes, lung, heart, bladder, adrenal gland and brain. Some hepatic and renal vessels contained neoplastic emboli (Fig. 1). There was extensive infiltration of the liver, kidneys and adrenal

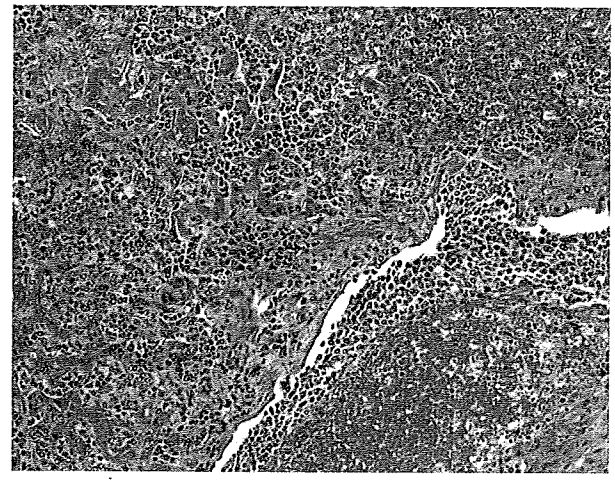

Fig. 1. Extensive infiltration of neoplastic cells into the hepatic parenchyma with associated degeneration and necrosis. A tumour embolus has formed in the central vein. HE. ×100.

glands by the same neoplastic population, with associated parenchymal degeneration or necrosis. Neoplastic cells were present in the spleen and lymph nodes, and in both tissues there was atrophy of lymphoid follicles. Sternal and femoral bone marrow contained many abnormal blast cells, with a marked reduction in normal haemopoietic tissue.

The neoplastic cells were generally poorly differentiated, with a medium-sized round nucleus, dense nuclear chromatin and either scant or abundant cytoplasm. Some larger cells had oval or pleomorphic macronuclei, whilst others were multinucleated, with a lower nuclear to cytoplasmic ratio (Fig. 2). There

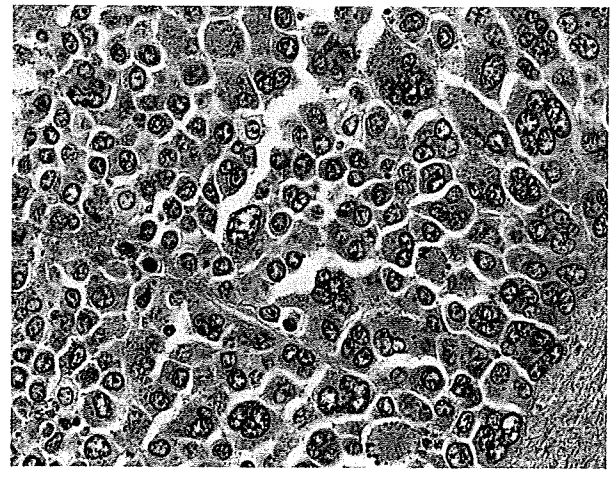

Fig. 2. Neoplastic cells within the liver. These vary greatly in size and are generally 2–3 times larger than normal lymphocytes. The majority of cells have large, round to oval nuclei with stippled chromatin and abundant cytoplasm. Some cells have macronuclei and others are multinucleated, with a lower nucleus to cytoplasmic ratio. HE. ×400.

were numerous abnormal mitoses. The majority of blast cells did not stain with PAS, but occasional individual cells were weakly stained. Masson's trichrome staining demonstrated severe fibrosis of the bone marrow (Fig. 3).

To further identify the neoplastic cells, immunohistochemical studies of femoral bone marrow, liver and kidney were performed. Sections were dewaxed, pre-treated with 0.5% H_2O_2 in methanol and then subjected to antigen retrieval with citric acid buffer (pH 6.0) and heating in an autoclave for 10 min at 121°C. Sections were then incubated with primary antibody overnight at 4°C. The primary antibodies employed were rabbit polyclonal antibodies specific for myeloperoxidase (Novocastra Laboratories, Newcastle, UK; 1 in 150 dilution); Von Willebrand Factor (Dako Cytomation, Denmark; 1 in 400 dilution); CD3 (Dako, 1 in 100 dilution); lysozyme (clone EC 3.2.1.17, Dako; 1 in 400 dilution) and monoclonal mouse antibodies specific for CD235a (clone JC159, Dako; 1 in 200 dilution); CD61-IIIa (cloneY2/51, Dako; 1 in 100 dilution); CD20 (clone L26, Dako; 1 in 100 dilution); HLA-DR alpha-chain (clone TAL.1B5, Dako; 1 in 40 dilution) and CD68 (clone KP1, Dako; 1 in 100 dilution). Following brief washes with buffer, the sections were incubated with the EnVision™ + Dual Link-HRP system (Dako) as secondary stage for 30 min. Labelling was "visualized" by treating the sections with the chromogen 3-3′-diaminobenzidine tetroxide (Dojin Kagaku, Japan) and H_2O_2. The sections were then counterstained with haematoxylin.

The majority of the neoplastic cells had granular cytoplasmic expression of the megakaryocyte-

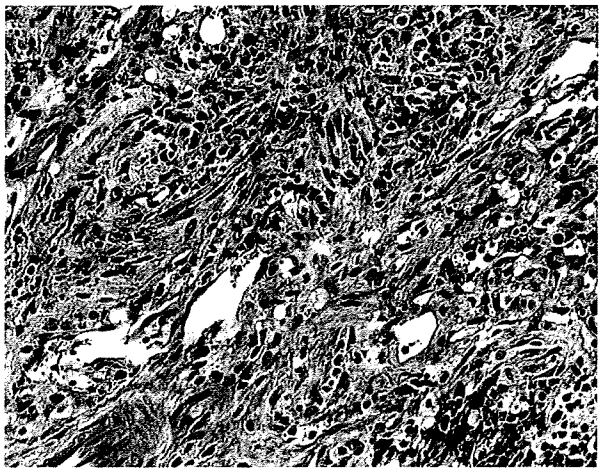

Fig. 3. Marked fibrosis (blue staining) is present within the bone marrow and admixed with neoplastic cells. Masson's trichrome. ×200.

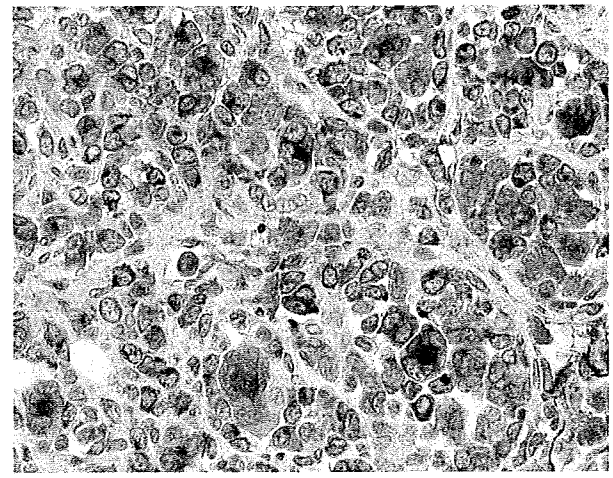

Fig. 4. Expression of Von Willebrand Factor by neoplastic cells within the bone marrow. IHC. ×400.

associated antigens Von Willebrand Factor (Fig. 4) and CD61-IIIa, but were negative for all other markers. On the basis of these findings, a diagnosis of AMKL (M7)-like disease with myelofibrosis was made. The neoplastic cells in AMKL often have granular cytoplasmic PAS staining when examined in a blood or a bone marrow smear (Wu *et al.*, 1996; Shukla *et al.*, 2004). The absence of significant PAS staining in the cells of the present case may relate to the formalin fixation process.

AMKL was first described as a subtype of acute myeloid leukaemia (AML) (von Boros and Korenyi, 1931) and was incorporated into the French–American–British (FAB) classification of AML as M7 (Bennett *et al.*, 1985). AMKL is rare, accounting for 3–5% of all human AML (Brunning *et al.*, 2001), but there is a higher incidence in children, partly due to an association with Down's syndrome (Athale *et al.*, 2001; Paredes-Aguilera *et al.*, 2003). Although AMKL is well characterized in man (Koike, 1984; Akahoshi *et al.*, 1987), in animals it has been reported only in the dog and cat (Colbatzky and Hermanns, 1993). Disrupted haematopoiesis leads to cytopenia, particularly thrombocytopenia, which becomes manifest as cutaneous petechiae, epistaxis and bleeding gums. In leukaemic patients there is often elevation of serum LDH concentration (Ferrara and Mirto, 1996). Since megakaryocytes, which store various growth factors in their alpha granules, are known to be involved in the pathogenesis of myelofibrosis, AMKL is frequently accompanied by myelofibrosis (Terui *et al.*, 1990). AMKL typically has a more guarded prognosis than other types of leukaemia (Athale *et al.*, 2001).

Differential diagnoses for AMKL include minimally differentiated AML (M0), pure erythroid

leukaemia (M6b) and acute lymphocytic leukaemia (ALL). M0, M6b and ALL are all generally negative for expression of myeloperoxidase in immunohistochemistry (IHC), as is AMKL. The neoplastic cells in AMKL occasionally have a lymphoblast-like appearance similar to M0 and ALL (Brunning *et al.*, 2001). Furthermore, neoplastic multinucleate cells are observed in both M6b and AMKL, and are often positively stained by PAS (Brunning *et al.*, 2001). Megakaryoblasts do not express myeloperoxidase, but are labelled by one or more of the megakaryocyte-associated antigens CD41, CD61 and Von Willebrand Factor (Brunning *et al.*, 2001; Daniel and Arber, 2001). The cytological and immunohistochemical features of the neoplastic population in the present case were not consistent with M0, M6b or ALL.

Further differential diagnoses for AMKL with myelofibrosis, as described in the present case, include acute panmyelosis with myelofibrosis (APMF), blastic transformation of chronic myeloid leukaemia (CML) or idiopathic myelofibrosis (IMF). APMF is characterized by multi-lineage myeloid proliferation, with a less numerous population of blast cells than in acute megakaryoblastic leukaemia (Orazi *et al.*, 2005). The cells in APMF do not express megakaryocyte-related antigens, which is inconsistent with the findings in the present case. CML is a clonal bone marrow stem cell disorder with proliferation of mature granulocytes (Travis *et al.*, 1987; Bourantas *et al.*, 1998) whereas IMF is a clonal myeloproliferative disorder that is characterized by abnormal deposition of collagen within the bone marrow (Hirose *et al.*, 2001). Human patients with CML or IMF also develop terminal blastic transformation, and these blast cells have frequently been identified as megakaryoblasts (Travis *et al.*, 1987; Bourantas *et al.*, 1998; Hirose *et al.*, 2001). Although the present case most likely represents AMKL with myelofibrosis, it is difficult to entirely exclude the alternative interpretation of blastic transformation of CML or IMF. For this reason, the present case has been described as an AMKL (M7)-like disease.

To our knowledge, this is the first case of spontaneously arising AMKL-like disease in non-human primates. The affected monkey had SRV/D infection, which may have contributed to the development of the neoplastic disease (Guzman *et al.*, 1999). Alternatively, a genetic mechanism may be proposed as humans with Down's syndrome have predisposition to the development of AMKL associated with a somatic mutation in the gene encoding the GATA1 transcription factor protein (Shimizu *et al.*, 2008). Further cases of such leukaemia in non-human primates should be subject to genetic investigation.

Acknowledgments

This study was supported by the Tsukuba Primate Research Center, National Institute of Biomedical Innovation, Japan.

References

Akahoshi, M., Oshimi, K., Mizoguchi, H., Okada, M., Enomoto, Y. and Watanabe, Y. (1987). Myeloproliferative disorders terminating in acute megakaryoblastic leukemia with chromosome 3q26 abnormality. *Cancer*, **60**, 2654–2661.

Athale, U. H., Razzouk, B. I., Raimondi, S. C., Tong, X., Behm, F. G., Head, D. R., Srivastava, D. K., Rubnitz, J. E., Bowman, L., Pui, C. H. and Ribeiro, R. C. (2001). Biology and outcome of childhood acute megakaryoblastic leukemia: a single institution's experience. *Blood*, **97**, 3727–3732.

Bennett, J. M., Catovsky, D., Daniel, M. T., Flandrin, G., Galton, D. A., Gralnick, H. R. and Sultan, C. (1985). Criteria for the diagnosis of acute leukemia of megakaryocyte lineage (M7). A report of the French–American–British Cooperative Group. *Annals of Internal Medicine*, **103**, 460–462.

von Boros, J. and Korenyi, A. (1931). Uber einen fall von akuter megakaryocyblasten-leukamie, zugleich einige bemerkungen zum problem der akuten leukemie. *Zeitschrift für Klinische Medizin*, **118**, 679–718.

Bourantas, K. L., Repousis, P., Tsiara, S., Christou, L., Konstantinidou, P. and Bai, M. (1998). Chronic myelogenous leukemia terminating in acute megakaryoblastic leukemia. Case report. *Journal of Experimental and Clinical Cancer Research*, **17**, 243–245.

Brunning, R. D., Matutes, E., Flandrin, G., Vardiman, J., Bennett, J., Head, D. and Harris, N. L. (2001). Acute myeloid leukemias. Pathology and genetics of tumours of haematopoietic and lymphoid tissues. In: *World Health Organization Classification of Tumors*, E. S. Jaffe, N. L. Harris, H. Stein and J. W. Vardiman, Eds, IARC Press, Lyon, pp. 77–105.

Colbatzky, F. and Hermanns, W. (1993). Acute megakaryoblastic leukemia in one cat and two dogs. *Veterinary Pathology*, **30**, 186–194.

Daniel, A. and Arber, M. D. (2001). Realistic pathologic classification of acute myeloid leukemias. *American Journal of Clinical Pathology*, **115**, 552–560.

Ferrara, F. and Mirto, S. (1996). Serum LDH value as a predictor of clinical outcome in acute myelogenous leukaemia of the elderly. *British Journal of Haematology*, **92**, 627–631.

Fortgang, I. S., Didier, P. J. and Levy, L. S. (2000). B-cell leukemia in a rhesus macaque (*Macaca mulatta*) infected with simian immunodeficiency virus. *Leukemia and Lymphoma*, **37**, 657–662.

Guzman, R. E., Kerlin, R. L. and Zimmerman, T. E. (1999). Histologic lesions in cynomolgus monkeys (*Macaca fascicularis*) naturally infected with simian retrovirus type D: comparison of seropositive, virus-positive, nd uninfected animals. *Toxicologic Pathology*, **27**, 672–677.

Hara, M., Kikuchi, T., Ono, F., Takano, J., Ageyama, N., Fujimoto, K., Terao, K., Baba, T. and Mukai, R. (2005). Survey of captive cynomolgus macaque colonies for SRV/D infection using polymerase chain reaction assays. *Comparative Medicine*, **55**, 145–149.

Hirose, Y., Masaki, Y., Shimoyama, K., Sugai, S. and Nojima, T. (2001). Granulocytic sarcoma of megakaryoblastic differentiation in the lymph nodes terminating as acute megakaryoblastic leukemia in a case of chronic idiopathic myelofibrosis persisting for 16 years. *European Journal of Haematology*, **67**, 194–198.

Hubbard, G. B., Moné, J. P., Allan, J. S., Davis, K. J., 3rd, Leland, M. M., Banks, P. M. and Smir, B. (1993). Spontaneously generated non-Hodgkin's lymphoma in twenty-seven simian T-cell leukemia virus type 1 antibody-positive baboons (*Papio species*). *Laboratory Animal Science*, **43**, 301–309.

Koike, T. (1984). Megakaryoblastic leukemia: the characterization and identification of megakaryoblasts. *Blood*, **64**, 683–692.

Orazi, A., O'Malley, D. P., Jiang, J., Vance, G. H., Thomas, J., Czader, M., Fang, W., An, C. and Banks, P. M. (2005). Acute panmyelosis with myelofibrosis: an entity distinct from acute megakaryoblastic leukemia. *Modern Pathology*, **18**, 603–614.

Paramastri, Y. A., Wallace, J. M., Salleng, K. J., Wilkinson, L. M., Malarkey, D. E. and Cline, J. M. (2002). Intracranial lymphomas in simian retrovirus-positive *Macaca fascicularis*. *Veterinary Pathology*, **39**, 399–402.

Paredes-Aguilera, R., Romero-Guzman, L., Lopez-Santiago, N. and Trejo, R. A. (2003). Biology, clinical, and hematologic features of acute megakaryoblastic leukemia in children. *American Journal of Hematology*, **73**, 71–80.

Shimizu, R., Engel, J. D. and Yamamoto, M. (2008). GATA1-related leukaemias. *Nature Reviews Cancer*, **8**, 279–287.

Shukla, J., Rai, S. and Singh, V. P. (2004). Acute megakaryoblastic leukaemia: a clinico-haematological profile of five cases. *Indian Journal of Pathology and Microbiology*, **47**, 266–268.

Terui, T., Niitsu, Y., Mahara, K., Fujisaki, Y., Urushizaki, Y., Mogi, Y., Kohgo, Y., Watanabe, N., Ogura, M. and Saito, H. (1990). The production of transforming growth factor-beta in acute megakaryoblastic leukemia and its possible implications in myelofibrosis. *Blood*, **75**, 1540–1548.

Travis, W. D., Li, C. Y., Banks, P. M. and Nichols, W. L. (1987). Megakaryoblastic transformation of chronic granulocytic leukemia. *Cancer*, **60**, 193–200.

Wu, C. D., Medeiros, L. J., Miranda, R. N., Mark, H. F. and Rintels, P. (1996). Chronic myeloid leukemia manifested during megakaryoblastic crisis. *Southern Medical Journal*, **89**, 422–427.

[*Received, September 5th, 2008*
Accepted, November 19th, 2008]

IL-4/IL-13 antagonist DNA vaccination successfully suppresses Th2 type chronic dermatitis

T. Morioka, K. Yamanaka, H. Mori, Y. Omoto, K. Tokime, M. Kakeda, I. Kurokawa, E.C. Gabazza,* A. Tsubura,† Y. Yasutomi‡ and H. Mizutani

Department of Dermatology and *Department of Immunology, Mie University, Graduate School of Medicine, 2-174 Edobashi, Tsu, Mie 514-8507, Japan
†Department of Pathology II, Kansai Medical University, Moriguchi, Osaka 570-8507, Japan
‡Laboratory of Immunoregulation and Vaccine Research, Tsukuba Primate Research Center, National Institute of Biomedical Innovation, Tsukuba, Ibaraki 305-0843, Japan

Correspondence
Hitoshi Mizutani.
E-mail: h-mizuta@clin.medic.mie-u.ac.jp

Accepted for publication
17 November 2008

Key words
atopic dermatitis, contact hypersensitivity, DNA vaccine, IL-4 mutant

Conflicts of interest
None declared.

DOI 10.1111/j.1365-2133.2009.09069.x

Summary

Background Atopic dermatitis (AD) is a chronic disease with a Th2-type-cytokine dominant profile. Several cytokines and related peptides have been used for the treatment of AD but they were ineffective because of their limited biological half-life. We have recently developed a highly efficient mouse dominant negative interleukin (IL)-4/IL-13 antagonist (IL-4DM), which blocks both IL-4 and IL-13 signal transductions.

Objective To examine the effects of IL-4DM in vivo in an AD model induced by the repeated exhibition of oxazolone (OX).

Methods Plasmid DNA was injected intraperitoneally to cause an experimental AD-like dermatitis. The effect was evaluated by ear thickness, histological findings, and mast cells counts in the inflamed skin. The plasma IgE and histamine levels were measured. Cytokine production in skin and splenocytes were also analysed.

Results Mice treated with control plasmid developed marked dermatitis with mast cells and eosinophil infiltration, and had increased plasma IgE and histamine levels with a Th2 type splenocyte cytokine profile. Treatment with mouse IL-4 DNA augmented the ear swelling and thickness with an increased dermal eosinophil count, plasma histamine level, and production of splenocyte IL-4. However, IL-4DM treatment successfully controlled the dermatitis, decreased the mast cell and eosinophil count, and suppressed plasma IgE and histamine levels. Splenocytes produced an increased level of IFN-γ.

Conclusion These data showed that the simultaneous suppression of IL-4/IL-13 signals successfully controlled Th2-type chronic dermatitis. IL-4DM DNA treatment is a potent therapy for AD and related diseases.

Interleukin (IL)-4 plays a central role in Th2-cytokine-dominant inflammatory skin diseases such as atopic dermatitis (AD).[1–3] IL-4 is responsible for the differentiation of allergen-specific Th2 cells together with its closely related cytokine IL-13 for the class switching of activated B cells to IgE-producing cells. The effects of IL-13 are similar to IL-4 on B cells, monocytes, and other cell types, but T cells appear to lack an IL-13 binding receptor component and do not respond to IL-13.[4] The structural basis for the overlapping functions of IL-4 and IL-13 is a shared receptor subunit, and IL-4Rα organizes intracellular signals in response to both cytokines.[5,6] Signal transduction is induced by heterodimerization of the IL-4Rα with a second subunit; which may vary according to the cell types. The specific inhibition of IL-4 can be achieved by antagonistic IL-4 mutants. Variants of human IL-4 that bind to the receptor subunit IL-4Rα, but not to the other subunit γ-chain (γc) or IL-13Rα1 are competitive antagonists of IL-4.[7,8] IL-13 is inhibited by similar variants, which form unproductive complexes with IL-4Rα.[5,9] The single-site human IL-4 mutant Y124D has been used as an IL-4/IL-13 inhibitor in various studies,[7–17] but this variant retains some residual agonistic activity, which could be relevant for in vivo applications.[7,8] In contrast, IL-4 and IL-13 double mutant R121D/Y124D lacks detectable activity and appears to be an effective antagonist for human IL-4 and IL-13.[5,18]

We have recently developed a highly efficient murine IL-4 antagonist DNA (IL-4DM), in which the amino acids glutamine 116 and tyrosine 119 were changed for aspartic acid.[19] This murine mutant DNA is analogous to the R121D/Y124D double mutant. IL-4DM binds with high affinity to the murine